The probe technique far from equilibrium: Magnetic field symmetries of nonlinear transport

Salil Bedkihal[1], Malay Bandyopadhyay[2], Dvira Segal[1]
[1] *Chemical Physics Theory Group, Department of Chemistry, University of Toronto, 80 Saint George St. Toronto, Ontario, Canada M5S 3H6 and*
[2] *School of Basic Sciences, Indian Institute of Technology Bhubaneswar, 751007, India*
(Dated: November 7, 2013)

The probe technique is a simple mean to incorporate elastic and inelastic processes into quantum transport problems. Using numerical simulations, we demonstrate that this tool can be employed beyond the analytically tractable linear response regime, providing a stable solution for the probe parameters: temperature and chemical potential. Adopting four probes: dephasing, voltage, temperature, and voltage-temperature, mimicking different elastic and inelastic effects, we provide a systematic analysis of magnetic field and gate voltage symmetries of charge current and heat current in Aharonov-Bohm interferometers, potentially far from equilibrium. Considering electron current, we prove that in the linear response regime inelastic scattering processes do not break the Onsager symmetry. Beyond linear response, even (odd) conductance terms obey an odd (even) symmetry with the threading magnetic flux, as long as the system acquires a spatial inversion symmetry. When spatial asymmetry is introduced, particle-hole symmetry assures that nonlinear conductance terms maintain certain symmetries with respect to magnetic field and gate voltage. These analytic results are supported by numerical simulations. Analogous results are obtained for the electron heat current. Finally, we demonstrate that a double-dot Aharonov-Bohm interferometer can act as a charge rectifier when two conditions are met simultaneously: (i) many-body effects are included, here in the form of inelastic scattering, and (ii) time reversal symmetry is broken.

PACS numbers: 73.23.-b,73.63.-b,05.60.-k

I. INTRODUCTION

Phase-breaking and energy dissipation processes arise due to the interaction of electrons with other degrees of freedom, e.g., with electrons, phonons, and defects. While an understanding of such effects, from first principles, is the desired objective of numerous computational approaches[1], simple analytical treatments are advantageous as they allow one to gain insights into transport phenomenology. The markovian quantum master equation and its variants (Lindblad, Redfield) is simple to study and interpret[2], and as such it has been extensively adopted in studies of charge, spin, exciton, and heat transport. It can be derived systematically, from projection operator techniques[3], and phenomenologically by introducing damping terms into the matrix elements of the reduced density matrix, to include dephasing and inelastic processes into the otherwise coherent dynamics.

Büttiker's probe technique[4–6] and its modern extensions to thermoelectric problems[7–10], atomic-level thermometry[11], and beyond linear response situations[12–16] present an alternative route for introducing decoherence and inelastic processes into coherent conductors. The probe is an electronic component[17], and it allows one to obtain information about local variables, chemical potential and temperature, deep within the conductor. When coupled strongly to the system, the probe can alter intrinsic transport mechanisms.

The probe technique can be exercised in several different ways, to induce distinct effects: *Elastic dephasing* processes are implemented by incorporating a "dephasing probe", enforcing the requirement that the net charge current towards the probe terminal, at any given energy, vanishes[18,19]. Inelastic *heat dissipative* effects are included by a "voltage probe", by demanding that the total-net charge current to the probe terminal nullifies[4–6]. This process dissipates heat since electrons leaving the system to the probe re-enter the conductor after being thermalized. In the complementary "temperature probe" *charge leakage* is allowed at the probe, but the probe temperature is tuned such that the net heat current at the probe is nil[20]. The "voltage-temperature probe", also referred to as a "thermometer", requires both charge cur-

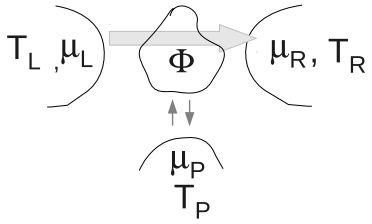

FIG. 1: Scheme of our setup. The horizontal arrow stands for the charge current across the conductor. The two parallel arrows represent currents into and from the P terminal, serving to induce elastic, inelastic, and dissipative effects. The parameters of the probe μ_P and T_P are determined in a self consistent manner, to satisfy the respective probe condition.

rent and heat current at the probe to vanish. In this case inelastic - energy exchange effects are allowed on the probe, but heat dissipation and charge leakage effects are excluded.

The probe technique has been used in different applications, particularly for the exploration of the ballistic to diffusive (Ohm's law and Fourier's law) crossover in electronic[5,21] and phononic conductors[22–25]. More recently, the effect of thermal rectification has been studied in phononic systems by utilizing the temperature probe as a mean to incorporate effective anharmonicity[12–14,26]. A full-counting statistics analysis of conductors including dephasing and voltage probes has been carried out in Ref.[27] The probe parameters, temperature and chemical potential, can be derived analytically when the conductor is set close to equilibrium[4,7,17]. Far from equilibrium, while these parameters can be technically defined and their uniqueness[15] allows for a physical interpretation, an exact analytic solution is missing. However, recent studies have demonstrated that iterative numerical schemes can reach a stable solution for the temperature probe[13,16]. These techniques have been then used for following phononic heat transfer in the deep quantum limit, far from equilibrium[13,16].

The present study is focused on the application of the probe technique to quantum open system problems in far-from-equilibrium situations. The Onsager-Casimir symmetry relations[28] are satisfied in phase-coherent conductors, reflecting the microreversibility of the scattering matrix. In Aharonov-Bohm interferometers with conserved electron current this symmetry is displayed by the "phase rigidity" of the (linear) conductance oscillations with the magnetic field B, $G_1(B) = G_1(-B)$[29,30]. Beyond linear response, the phase symmetry of the conductance is not enforced, and several experiments[31–40] have demonstrated its breakdown. Supporting theoretical works have elucidated the role of many-body interactions in the system[41–46], typically approaching the problem by calculating the screening potential within the conductor in a self-consistent manner, a procedure often limited to low-order conduction terms[41,43,45].

Our objective here is to provide a *systematic and comprehensive* analysis of the role of different types of probes on transport symmetries in nonlinear conductors. We want to understand the role of elastic dephasing, heat dissipation, and charge leakage processes on symmetries of charge current, rectification, and heat current in two-terminal conductors, with respect to the magnetic field, temperature bias, and voltage bias. Specifically, our main goal is to develop, and analyze the breakdown, of symmetry relations for nonlinear transport beyond the Onsager-Casimir result in the presence of incoherent effects.

Our study of transport behavior beyond linear response further exposes sufficient conditions for the onset of the charge current rectification (diode) effect, referring to the situation where the magnitude of the current differs when the bias polarity is reversed. This effect, of fundamental and practical interest, is realized by combining many-body interactions with a broken symmetry: broken spatial inversion symmetry or a broken time reversal symmetry. Rectifiers of the first type have been extensively investigated theoretically and experimentally, including electronic rectifiers, thermal rectifiers[47] and acoustic rectifiers[48]. In parallel, optical and spin rectifiers were designed based on a broken time reversal symmetry, recently realized e.g. by engineering parity-time meta-materials[49]. The model system investigated in this work, a double-dot AB junction, offers a feasible setup for devising broken time reversal rectifiers.

This work extends our recent contribution[50] in several significant ways: (i) We consider here four different probes (dephasing, voltage, temperature and voltage-temperature) and demonstrate with numerical simulations a stable solution and a facile convergence for the probe parameters far from equilibrium. (ii) While in Ref.[50] we have focused on the development of magnetic-field symmetry relations when the device is geometrically symmetric, here we obtain more general relations, valid in the presence of spatial asymmetries, a result of particle-hole symmetry. (iii) We discuss the operation of the double-dot interferometer, susceptible to inelastic effects, as a charge rectifier, when time reversal symmetry is broken. (iv) We derive symmetry relations for nonlinear heat transfer in the presence of charge leakage.

The paper is organized as follows. In Sec. II we provide expressions for the charge and heat currents in the Landauer formalism and discuss four types of probes, inducing different effects. Sec. III introduces the main observables of interest and summarizes our principal results. Sec. IV covers situations that fulfill phase rigidity. Magnetic field symmetry relations in a spatially symmetric setup are derived in Sec. V. Magnetic field- gate voltage symmetries, valid for generic double-dot AB interferometer models, are presented in Sec. VI. Supporting numerical simulations are included in Sec. VII. Sec. VIII concludes. For simplicity, we set e=1, $h = 1$ and $k_B = 1$. The words "diode" and "rectifier" are used interchangeably in this work, referring to a dc-rectifier.

II. FORMALISM

In the scattering formalism of Landauer and Büttiker[4,51–53], interactions between particles are neglected. Considering a multi-terminal setup, one can express the charge current from the ν to the ξ terminal in terms of the transmission probability $\mathcal{T}_{\nu,\xi}(\epsilon)$, a function which depends on the energy of the incident electron,

$$I_\nu(\phi) \;=\; \int_{-\infty}^{\infty} d\epsilon \Big[\sum_{\xi\neq\nu} \mathcal{T}_{\nu,\xi}(\epsilon,\phi) f_\nu(\epsilon) - \sum_{\xi\neq\nu} \mathcal{T}_{\xi,\nu}(\epsilon,\phi) f_\xi(\epsilon) \Big]. \tag{1}$$

The magnetic field is introduced via an Aharonov-Bohm flux Φ applied through the conductor, with the magnetic

phase $\phi = 2\pi\Phi/\Phi_0$, $\Phi_0 = h/e$ is the magnetic flux quantum. The transmission function can be written in terms of the Green's function of the system and the self energy matrices. Explicit expressions for a particular model are included in Sec. VI. The Fermi-Dirac distribution function $f_\nu(\epsilon) = [e^{\beta_\nu(\epsilon-\mu_\nu)}+1]^{-1}$ is defined in terms of the chemical potential μ_ν and the inverse temperature β_ν.

Our analysis below relies on two basic relations. First, the transmission coefficient from the ξ to the ν reservoir obeys reciprocity, given the unitarity and time reversal symmetry of the scattering matrix,

$$\mathcal{T}_{\xi,\nu}(\epsilon,\phi) = \mathcal{T}_{\nu,\xi}(\epsilon,-\phi). \tag{2}$$

Second, the total probability is conserved,

$$\sum_{\xi\neq\nu}\mathcal{T}_{\xi,\nu}(\epsilon,\phi) = \sum_{\xi\neq\nu}\mathcal{T}_{\nu,\xi}(\epsilon,\phi). \tag{3}$$

A proof for the second relation, in the presence of a probe, is included in Appendix A of Ref.[45], based on the Green's function formalism.

In this work we consider a setup including three terminals, L, R and P, where the P terminal serves as the probe, see Fig. 1. We focus below on the steady-state charge current from the L reservoir to the central system (I_L) and from the probe to the system (I_P),

$$\begin{aligned} I_L(\phi) &= \int_{-\infty}^{\infty} d\epsilon\Big[\mathcal{T}_{L,R}(\epsilon,\phi)f_L(\epsilon) - \mathcal{T}_{R,L}(\epsilon,\phi)f_R(\epsilon) \\ &+ \mathcal{T}_{L,P}(\epsilon,\phi)f_L(\epsilon) - \mathcal{T}_{P,L}(\epsilon,\phi)f_P(\epsilon,\phi)\Big], \end{aligned} \tag{4}$$

$$\begin{aligned} I_P(\phi) &= \int_{-\infty}^{\infty} d\epsilon\Big[\mathcal{T}_{P,L}(\epsilon,\phi)f_P(\epsilon,\phi) - \mathcal{T}_{L,P}(\epsilon,\phi)f_L(\epsilon) \\ &+ \mathcal{T}_{P,R}(\epsilon,\phi)f_P(\epsilon,\phi) - \mathcal{T}_{R,P}(\epsilon,\phi)f_R(\epsilon)\Big]. \end{aligned} \tag{5}$$

Similarly, we can write the heat current at the $\nu = L$ terminal as

$$\begin{aligned} Q_L(\phi) = \int_{-\infty}^{\infty} d\epsilon\,(\epsilon-\mu_L)\Big[&\mathcal{T}_{L,R}(\epsilon,\phi)f_L(\epsilon) \\ -\mathcal{T}_{R,L}(\epsilon,\phi)f_R(\epsilon) + \mathcal{T}_{L,P}(\epsilon,\phi)f_L(\epsilon) &- \mathcal{T}_{P,L}(\epsilon,\phi)f_P(\epsilon,\phi)\Big]. \end{aligned} \tag{6}$$

The heat current at the probe is given by an analogous expression. The probe distribution function is determined by the probe condition. It is generally influenced by the magnetic flux, as we demonstrate in Secs. IV-VII.

For convenience, we simplify next our notation. First, we drop the reference to the energy of incoming electrons ϵ in both transmission functions and distribution functions. Second, since all integrals are evaluated between $\pm\infty$, we do not put the limits explicitly. Third, unless otherwise mentioned f_P, μ_P and all transmission coefficients are evaluated at the phase $+\phi$, thus we do not explicitly write the phase variable. If we do need to consider e.g. the transmission function $\mathcal{T}_{\nu,\xi}(-\phi)$, we write instead the complementary expression, $\mathcal{T}_{\xi,\nu}(\phi)$.

Dephasing probe. We implement elastic dephasing effects by demanding that the energy-resolved particle current diminishes in the probe,

$$I_P(\epsilon) = 0 \quad \text{with} \quad I_P = \int I_P(\epsilon)d\epsilon. \tag{7}$$

Using this condition, Eq. (5) provides a closed form for the corresponding (flux-dependent) probe distribution, not necessarily in the form of a Fermi function.

Voltage probe. We introduce dissipative inelastic effects into the conductor using the voltage probe technique. The three reservoirs are maintained at the same inverse temperature β_a, but the L and R chemical potentials are made distinct, $\mu_L \neq \mu_R$. Our objective is to obtain μ_P, and it is reached by demanding that the net-total particle current flowing into the P reservoir diminishes,

$$I_P = 0. \tag{8}$$

This choice allows for dissipative energy exchange processes to take place within the probe. In the linear response regime Eq. (5) can be used to derive an analytic expression for μ_P. In far-from-equilibrium situations we obtain the unique[15] chemical potential of the probe numerically, using the Newton-Raphson method[54]

$$\mu_P^{(k+1)} = \mu_P^{(k)} - I_P(\mu_P^{(k)})\left[\frac{\partial I_P(\mu_P^{(k)})}{\partial\mu_P}\right]^{-1}. \tag{9}$$

The current $I_P(\mu_P^{(k)})$ and its derivative are evaluated from Eq. (5) using the probe (Fermi) distribution with $\mu_P^{(k)}$. Note that the self-consistent probe solution varies with the magnetic flux.

Temperature probe. In this scenario the three reservoirs L,R,P are maintained at the same chemical potential μ_a, but the temperature at the L and R terminals are made different, $T_L \neq T_R$. The probe temperature $T_P = \beta_P^{-1}$ is determined by requiring the net heat current at the probe to satisfy

$$Q_P = 0. \tag{10}$$

This constraint allows for charge leakage into the probe since we do not require Eq. (8) to hold. We can obtain the temperature T_P numerically by following an iterative procedure,

$$T_P^{(k+1)} = T_P^{(k)} - Q_P(T_P^{(k)})\left[\frac{\partial Q_P(T_P^{(k)})}{\partial T_P}\right]^{-1}. \tag{11}$$

The probe temperature varies with the applied flux ϕ, see Appendix B.

Voltage-temperature probe. This probe acts as an electron thermometer at weak coupling. We set the temperatures $T_{L,R}$ and the potentials $\mu_{L,R}$, and demand that

$$I_P = 0 \quad \text{and } Q_P = 0. \tag{12}$$

In other words, the charge and heat currents in the conductor satisfy $I_L = -I_R$ and $Q_L = -Q_R$, since neither charge nor heat are allowed to dissipate at the probe. Analytic results can be obtained in the linear response regime, see for example Refs.[7,21]. Beyond that, equation (12) can be solved self-consistently, to provide T_P and μ_P. This can be done by utilizing the two-dimensional Newton-Raphson method,

$$\begin{aligned}\mu_P^{(k+1)} &= \mu_P^{(k)} - D_{1,1}^{-1} I_P(\mu_P^{(k)}, T_P^{(k)}) - D_{1,2}^{-1} Q_P(\mu_P^{(k)}, T_P^{(k)}) \\ T_P^{(k+1)} &= T_P^{(k)} - D_{2,1}^{-1} I_P(\mu_P^{(k)}, T_P^{(k)}) - D_{2,2}^{-1} Q_P(\mu_P^{(k)}, T_P^{(k)}),\end{aligned} \tag{13}$$

where the Jacobean D is re-evaluated at every iteration,

$$D(\mu_P, T_P) \equiv \begin{pmatrix} \frac{\partial I_P(\mu_P,T_P)}{\partial \mu_P} & \frac{\partial I_P(\mu_P,T_P)}{\partial T_P} \\ \frac{\partial Q_P(\mu_P,T_P)}{\partial \mu_P} & \frac{\partial Q_P(\mu_P,T_P)}{\partial T_P} \end{pmatrix}$$

We emphasize that besides the case of the dephasing probe, the function $f_P(\phi)$ is forced to take the form of a Fermi-Dirac distribution function in the other probe models.

III. SYMMETRY MEASURES AND MAIN RESULTS

In the main body of this paper we restrict ourselves to voltage-biased junctions, $\mu_L \neq \mu_R$, while setting $T_a = \beta_a^{-1} = T_L = T_R$. We also limit our focus to charge conserving systems satisfying

$$I(\phi) \equiv I_L(\phi) = -I_R(\phi), \tag{14}$$

and study the role of elastic dephasing (dephasing probe) and dissipative (voltage probe) and non-dissipative (voltage-temperature probe) inelastic effects on the charge transport symmetries with magnetic flux. In Appendix B we complement this analysis by considering a temperature-biased heat-conserving junction, $T_L \neq T_R$, $\mu_a = \mu_L = \mu_R$ and $Q_L = -Q_R$. We then study the phase symmetry of the heat current, allowing for charge leakage in the probe. We do not study the thermoelectric effect in this work.

We now define several measures for quantifying phase symmetry in a voltage-biased three-terminal junction satisfying Eq. (14). Expanding the charge current in powers of the bias $\Delta\mu$ we write[55]

$$I(\phi) = G_1(\phi)\Delta\mu + G_2(\phi)(\Delta\mu)^2 + G_3(\phi)(\Delta\mu)^3 + ... \tag{15}$$

with $G_{n>1}$ as the nonlinear conductance coefficients. In this work we study relations between two quantities: a measure for the magnetic field asymmetry

$$\Delta I(\phi) \equiv \frac{1}{2}[I(\phi) - I(-\phi)], \tag{16}$$

and the dc-rectification current,

$$\begin{aligned}\mathcal{R}(\phi) &\equiv \frac{1}{2}[I(\phi) + \bar{I}(\phi)] \\ &= G_2(\phi)(\Delta\mu)^2 + G_4(\phi)(\Delta\mu)^4 + ...\end{aligned} \tag{17}$$

with $\bar{I}$ defined as the current obtained upon interchanging the chemical potentials of the two terminals. We also study the behavior of odd conductance terms,

$$\begin{aligned}\mathcal{D}(\phi) &\equiv \frac{1}{2}[I(\phi) - \bar{I}(\phi)] \\ &= G_1(\phi)\Delta\mu + G_3(\phi)(\Delta\mu)^3 + ...\end{aligned} \tag{18}$$

For a non-interacting system we expect the relation

$$I(\phi) = -\bar{I}(-\phi) \tag{19}$$

to hold. Combined with Eq. (15) we immediately note that $G_{2n+1}(\phi) = G_{2n+1}(-\phi)$ and $G_{2n}(\phi) = -G_{2n}(-\phi)$ with n as an integer. We show below that these relations are obeyed in a symmetric junction even when many-body interactions (inelastic scattering) are included. This result is not trivial since the included many-body interactions are reflected by probe parameters which depend on the applied bias in a nonlinear manner and the magnetic phase in an asymmetric form, thus, we cannot assume Eq. (19) to immediately hold.

Using Eq. (4), we express the deviation from the magnetic field symmetry as

$$\begin{aligned}\Delta I &= \frac{1}{2}\int \left[\mathcal{T}_{L,R} - \mathcal{T}_{R,L}\right](f_L + f_R)d\epsilon \\ &+ \frac{1}{2}\int \left[\mathcal{T}_{L,P} - \mathcal{T}_{P,L}\right] f_L d\epsilon \\ &+ \frac{1}{2}\int \left[\mathcal{T}_{L,P} f_P(-\phi) - \mathcal{T}_{P,L} f_P(\phi)\right] d\epsilon\end{aligned} \tag{20}$$

We use the probability conservation, Eq. (3), and simplify this relation,

$$\begin{aligned}\Delta I &= \frac{1}{2}\int \left[\mathcal{T}_{L,R} - \mathcal{T}_{R,L}\right] f_R d\epsilon \\ &+ \frac{1}{2}\int \left[\mathcal{T}_{L,P} f_P(-\phi) - \mathcal{T}_{P,L} f_P(\phi)\right] d\epsilon.\end{aligned} \tag{21}$$

Since $I_L = -I_R$, the rectification current can be written in two equivalent forms,

$$\begin{aligned}\mathcal{R} &= \frac{1}{2}\int \mathcal{T}_{P,L}(f_L + f_R - f_P(\phi) - \bar{f}_P(\phi))d\epsilon \\ &= -\frac{1}{2}\int \mathcal{T}_{P,R}(f_L + f_R - f_P(\phi) - \bar{f}_P(\phi))d\epsilon,\end{aligned} \tag{22}$$

with $\bar{f}_P$ as the probe distribution when the biases μ_L and μ_R are interchanged. We can also weight these expressions and adopt a symmetric definition

$$\mathcal{R} = \int \frac{\mathcal{T}_{P,L} - \mathcal{T}_{P,R}}{4}(f_L + f_R - f_P(\phi) - \bar{f}_P(\phi))d\epsilon \tag{23}$$

The behavior of odd conductance terms can be similarly written as

$$\begin{aligned}\mathcal{D}(\phi) &= \frac{1}{2}\int\Big\{\left[\mathcal{T}_{L,R}+\mathcal{T}_{L,P}+\mathcal{T}_{R,L}\right](f_L-f_R)\\ &- \mathcal{T}_{P,L}[f_P(\phi)-\bar{f}_P(\phi)]\Big\}d\epsilon\\ &= -\frac{1}{2}\int\Big\{\left[\mathcal{T}_{L,R}+\mathcal{T}_{R,P}+\mathcal{T}_{R,L}\right](f_R-f_L)\\ &- \mathcal{T}_{P,R}[f_P(\phi)-\bar{f}_P(\phi)]\Big\}d\epsilon \qquad (24)\end{aligned}$$

Our results are organized by systematically departing from quantum coherent scenarios, the linear response regime, and spatially symmetric situations. The paper includes four parts, and we now summarize our main results:

(i) *Phase Rigidity.* In Sec. IV we discuss two scenarios that do obey the Onsager-Casimir symmetry relation $I(\phi)$=$I(-\phi)$: It is maintained in the presence of elastic dephasing effects even beyond linear response. This relation is also valid when inelastic scatterings are included, albeit only in the linear response regime. While these results are not new[52], we include this analysis here so as to clarify the role of inelastic effects in breaking the Onsager symmetry, beyond linear response.

(ii) *Magnetic field (MF) symmetry relations beyond linear response.* In Sec. V we derive magnetic-field symmetry relations that hold beyond linear response in *spatially symmetric* junctions susceptible to inelastic effects, $\mathcal{R}(\phi)=\Delta I(\phi)=-\mathcal{R}(-\phi)$ and $\mathcal{D}(\phi)=\mathcal{D}(-\phi)$. In other words, we show that odd (even) conductance terms are even (odd) in the magnetic flux. Note that "spatial" or "geometrical" symmetry refers here to the left-right mirror symmetry of the junction. Below we refer to these symmetries as the "MF symmetry relations" .

(iii) *Magnetic field-Gate voltage (MFGV) symmetry relations beyond linear response.* In Secs. VI-VII we focus on geometrically *asymmetric* setups, adopting the double dot AB interferometer as an example. While we demonstrate, using numerical simulations, the breakdown of the MF relations under spatial asymmetry, in Appendix A we prove that charge conjugation symmetry entails magnetic field-gate voltage symmetries: $\mathcal{R}(\epsilon_d,\phi)=-\mathcal{R}(-\epsilon_d,-\phi)$, and $\mathcal{D}(-\epsilon_d,-\phi)=\mathcal{D}(\epsilon_d,\phi)$, with ϵ_d as the double-dot energies. We refer below to these symmetries as the "MFGV symmetry relations" .

(iv) In Appendix B we prove that the heat current (within a heat-conserving setup) satisfies relations analogous to (i)-(iii).

IV. PHASE RIGIDITY AND ABSENCE OF RECTIFICATION

The Onsager-Casimir symmetry $I(\phi)=I(-\phi)$ is preserved under dephasing effects, implemented via a dephasing probe, even beyond the linear response regime. It is also satisfied in the presence of elastic and inelastic effects, implemented using the voltage probe technique, only as long the system is maintained in the linear response regime. These results have already been discussed in e.g., Ref.[52]. We detail these steps here so as to provide closed expressions for the probe parameters in the linear response regime.

A. Dephasing effects beyond linear response

Implementing the dephasing probe (7) we obtain the respective distribution

$$f_P(\phi)=\frac{\mathcal{T}_{L,P}f_L+\mathcal{T}_{R,P}f_R}{\mathcal{T}_{P,L}+\mathcal{T}_{P,R}}. \qquad (25)$$

We substitute this function into Eq. (21), the measure for phase asymmetry, and obtain

$$\begin{aligned}\Delta I &= \frac{1}{2}\int\left[\mathcal{T}_{L,R}-\mathcal{T}_{R,L}\right]f_R d\epsilon\\ &+ \frac{1}{2}\int\mathcal{T}_{L,P}\frac{\mathcal{T}_{P,L}f_L+\mathcal{T}_{P,R}f_R}{\mathcal{T}_{L,P}+\mathcal{T}_{R,P}}d\epsilon\\ &- \frac{1}{2}\int\mathcal{T}_{P,L}\frac{\mathcal{T}_{L,P}f_L+\mathcal{T}_{R,P}f_R}{\mathcal{T}_{P,L}+\mathcal{T}_{P,R}}d\epsilon \qquad (26)\end{aligned}$$

The denominators in these integrals are identical, see Eq. (3), thus we combine the last two terms into

$$\begin{aligned}\Delta I &= \frac{1}{2}\int\left[\mathcal{T}_{L,R}-\mathcal{T}_{R,L}\right]f_R d\epsilon\\ &+ \frac{1}{2}\int\frac{\left[\mathcal{T}_{L,P}\mathcal{T}_{P,R}-\mathcal{T}_{P,L}\mathcal{T}_{R,P}\right]f_R}{\mathcal{T}_{P,R}+\mathcal{T}_{P,L}}d\epsilon. \qquad (27)\end{aligned}$$

Utilizing Eq. (3) in the form $\mathcal{T}_{L,P}=\mathcal{T}_{P,L}+\mathcal{T}_{P,R}-\mathcal{T}_{R,P}$, we organize the numerator of the second integral, $(\mathcal{T}_{P,R}-\mathcal{T}_{R,P})(\mathcal{T}_{P,R}+\mathcal{T}_{P,L})f_R$. This results in

$$\begin{aligned}\Delta I &= \frac{1}{2}\int\left[\mathcal{T}_{L,R}-\mathcal{T}_{R,L}+\mathcal{T}_{P,R}-\mathcal{T}_{R,P}\right]f_R d\epsilon\\ &= \frac{1}{2}\int f_R\left[\sum_{\nu\neq R}\mathcal{T}_{\nu,R}-\sum_{\nu\neq R}\mathcal{T}_{R,\nu}\right]d\epsilon, \qquad (28)\end{aligned}$$

which is identically zero, given Eq. (3). This concludes our proof that dephasing effects, implemented via a dephasing probe, cannot break phase rigidity even in the nonlinear regime.

Following similar steps we show that elastic dephasing effects cannot bring about the effect of charge rectification even when the junction acquires spatial asymmetries. We substitute f_P into Eq. (4) and obtain

$$I_L=\int\left[F_L f_L-F_R f_R\right]d\epsilon \qquad (29)$$

with

$$F_L=\frac{\mathcal{T}_{L,R}(\mathcal{T}_{P,L}+\mathcal{T}_{P,R})+\mathcal{T}_{L,P}\mathcal{T}_{P,R}}{(\mathcal{T}_{P,L}+\mathcal{T}_{P,R})}. \qquad (30)$$

F_R is defined analogously, interchanging L by R. We now note the following identities,

$$\begin{aligned}&\mathcal{T}_{L,P}\mathcal{T}_{P,R} = [\mathcal{T}_{P,L}+\mathcal{T}_{P,R}-\mathcal{T}_{R,P}]\mathcal{T}_{P,R}\\&= (\mathcal{T}_{P,R}-\mathcal{T}_{R,P})(\mathcal{T}_{P,R}+\mathcal{T}_{P,L})+\mathcal{T}_{P,L}\mathcal{T}_{R,P}\\&= (\mathcal{T}_{R,L}-\mathcal{T}_{L,R})(\mathcal{T}_{P,R}+\mathcal{T}_{P,L})+\mathcal{T}_{P,L}\mathcal{T}_{R,P}\end{aligned} \quad (31)$$

Reorganizing the first and third lines we find that

$$\begin{aligned}&\mathcal{T}_{L,R}(\mathcal{T}_{P,R}+\mathcal{T}_{P,L})+\mathcal{T}_{L,P}\mathcal{T}_{P,R}\\&= \mathcal{T}_{R,L}(\mathcal{T}_{P,R}+\mathcal{T}_{P,L})+\mathcal{T}_{P,L}\mathcal{T}_{R,P}\end{aligned} \quad (32)$$

which immediately implies that $F_L = F_R$. This is turn leads to $I = -\bar{I}$, thus $\mathcal{R} = 0$. We conclude that the current only includes odd (linear and nonlinear) conductance terms under elastic dephasing, $I = \mathcal{D}(\phi) = \mathcal{D}(-\phi)$, and that phase rigidity is maintained even if spatial asymmetry is presented. This conclusion in valid under both applied voltage and temperature biases.

B. Inelastic effects in linear response

We introduce inelastic effects using the voltage probe technique. In the linear response regime we expand the Fermi functions of the three terminals around the equilibrium state $f_a(\epsilon) = [e^{\beta_a(\epsilon-\mu_a)}+1]^{-1}$,

$$f_\nu(\epsilon) = f_a(\epsilon) - (\mu_\nu - \mu_a)\frac{\partial f_a}{\partial \epsilon}. \quad (33)$$

The three terminals are maintained at the same temperature T_a. The derivative $\frac{\partial f_a}{\partial \epsilon}$ is evaluated at the equilibrium value μ_a. For simplicity we set $\mu_a = 0$. We enforce the voltage probe condition, $I_P = 0$, demanding that

$$\int \left[(\mathcal{T}_{P,L}+\mathcal{T}_{P,R})\, f_P(\phi) - \mathcal{T}_{L,P} f_L - \mathcal{T}_{R,P} f_R\right] d\epsilon = 0. \quad (34)$$

In linear response this translates to

$$\begin{aligned}0 \;=\; &\int \Big[(\mathcal{T}_{P,L}+\mathcal{T}_{P,R})\left(f_a - \mu_P(\phi)\frac{\partial f_a}{\partial \epsilon}\right)\\ &- \mathcal{T}_{L,P}\left(f_a - \mu_L\frac{\partial f_a}{\partial \epsilon}\right) - \mathcal{T}_{R,P}\left(f_a - \mu_R\frac{\partial f_a}{\partial \epsilon}\right)\Big] d\epsilon.\end{aligned} \quad (35)$$

For convenience, we apply the voltage in a symmetric manner, $\mu_L = -\mu_R = \Delta\mu/2$. We organize Eq. (35) and obtain the probe chemical potential, a linear function in $\Delta\mu$,

$$\mu_P(\phi) = \frac{\Delta\mu}{2}\frac{\int d\epsilon \frac{\partial f_a}{\partial \epsilon}\left(\mathcal{T}_{L,P}-\mathcal{T}_{R,P}\right)}{\int d\epsilon \frac{\partial f_a}{\partial \epsilon}\left(\mathcal{T}_{P,L}+\mathcal{T}_{P,R}\right)}. \quad (36)$$

We simplify this result by introducing a short notation for the conductance between the ν and ξ terminals,

$$G_{\nu,\xi}(\phi) \equiv \int d\epsilon \left(-\frac{\partial f_a}{\partial \epsilon}\right)\mathcal{T}_{\nu,\xi}(\epsilon,\phi). \quad (37)$$

This quantity fulfills relations analogous to Eqs. (2) and (3)[4]. For brevity, we do not write next the phase variable in G, evaluating it at the phase ϕ unless otherwise mentioned. The probe potential can now be compacted,

$$\mu_P(\phi) = \frac{\Delta\mu}{2}\frac{G_{L,P}-G_{R,P}}{G_{P,L}+G_{P,R}}. \quad (38)$$

Furthermore, in geometrically symmetric systems $\mathcal{T}_{R,P}(\epsilon,\phi) = \mathcal{T}_{P,L}(\epsilon,\phi)$, resulting in $G_{R,P}(\phi) = G_{P,L}(\phi)$ and

$$\mu_P(\phi) = \frac{\Delta\mu}{2}\frac{G_{L,P}(\phi)-G_{L,P}(-\phi)}{G_{L,P}(\phi)+G_{L,P}(-\phi)}. \quad (39)$$

Thus $\mu_P(\phi) = -\mu_P(-\phi)$ in linear response. Below we show that this symmetry does not hold far from equilibrium. We now expand Eq. (21) in the linear response regime

$$\begin{aligned}\Delta I \;=\; &\frac{1}{2}\int (\mathcal{T}_{L,R}-\mathcal{T}_{R,L})\left(f_a - \mu_R\frac{\partial f_a}{\partial \epsilon}\right)d\epsilon\\ &+ \frac{1}{2}\int\Bigg\{\mathcal{T}_{L,P}\left[f_a - \mu_P(-\phi)\frac{\partial f_a}{\partial \epsilon}\right]\\ &- \mathcal{T}_{P,L}\left[f_a - \mu_P(\phi)\frac{\partial f_a}{\partial \epsilon}\right]\Bigg\}d\epsilon.\end{aligned} \quad (40)$$

Utilizing the definition (37) we compact this expression,

$$\begin{aligned}\Delta I \;=\; &\frac{1}{2}\left(G_{L,R}-G_{R,L}\right)\mu_R\\ &- \frac{1}{2}\left[G_{P,L}\mu_P(\phi) - G_{L,P}\mu_P(-\phi)\right].\end{aligned} \quad (41)$$

Using Eq. (3), the first line can be rewritten as

$$I_1 = \frac{\Delta\mu}{4}\left(G_{L,P}-G_{P,L}\right). \quad (42)$$

The second line in Eq. (41) reduces to

$$\begin{aligned}I_2 \;&=\; -\frac{\Delta\mu}{4}G_{P,L}\frac{G_{L,P}-G_{R,P}}{\mathcal{N}} + \frac{\Delta\mu}{4}G_{L,P}\frac{G_{P,L}-G_{P,R}}{\mathcal{N}}\\ &=\; -\frac{\Delta\mu}{4}\frac{G_{L,P}G_{P,R}-G_{P,L}G_{R,P}}{\mathcal{N}}\end{aligned} \quad (43)$$

where we have introduced the short notation $\mathcal{N} \equiv G_{P,L}+G_{P,R}$. Now, we substitute $G_{L,P} = G_{P,L}+G_{P,R}-G_{R,P}$, and this allows us to write

$$\begin{aligned}I_2 \;&=\; -\frac{\Delta\mu}{4}\frac{(G_{P,R}-G_{R,P})(G_{P,R}+G_{P,L})}{\mathcal{N}}\\ &=\; -\frac{\Delta\mu}{4}(G_{P,R}-G_{R,P}).\end{aligned} \quad (44)$$

Combining $\Delta I = I_1 + I_2$, we reach

$$\begin{aligned}\Delta I \;&=\; -\frac{\Delta\mu}{4}\left(G_{P,R}-G_{R,P}-G_{L,P}+G_{P,L}\right)\\ &=\; -\frac{\Delta\mu}{4}\left(\sum_{\nu\neq P}G_{P,\nu} - \sum_{\nu\neq P}G_{\nu,P}\right)\end{aligned} \quad (45)$$

which is identically zero given the conductance conservation (3). It is trivial to note that no rectification takes place in the linear response regime, $\mathcal{R} = 0$.

V. BEYOND LINEAR RESPONSE: SPATIALLY SYMMETRIC SETUPS

In this section we consider the role of inelastic effects on the current symmetry in an AB interferometer, beyond the linear response regime. The probe condition $I_P = 0$ translates Eq. (5) into three relations,

$$\begin{aligned}\int d\epsilon(\mathcal{T}_{P,L}+\mathcal{T}_{P,R})f_P(\phi) &= \int d\epsilon(\mathcal{T}_{L,P}f_L+\mathcal{T}_{R,P}f_R)\\ \int d\epsilon(\mathcal{T}_{L,P}+\mathcal{T}_{R,P})f_P(-\phi) &= \int d\epsilon(\mathcal{T}_{P,L}f_L+\mathcal{T}_{P,R}f_R)\\ \int d\epsilon(\mathcal{T}_{P,L}+\mathcal{T}_{P,R})\bar{f}_P(\phi) &= \int d\epsilon\,(\mathcal{T}_{L,P}f_R+\mathcal{T}_{R,P}f_L)\end{aligned} \quad (46)$$

First, we consider the situation when time reversal symmetry is protected, with the magnetic phase given by multiples of 2π. Then, $\mathcal{T}_{\nu,\xi} = \mathcal{T}_{\xi,\nu}$, and particularly we note that $\mathcal{T}_{L,P} = \mathcal{T}_{P,L}$. Furthermore, in the model considered in Sec. VI, $\mathcal{T}_{P,L} = \chi\mathcal{T}_{P,R}$, with χ as an energy independent parameter, reflecting spatial asymmetry, see for example the discussion around Eq. (60). Using the voltage probe condition (46) we find that

$$\begin{aligned}&\int(\mathcal{T}_{P,L}+\mathcal{T}_{P,R})(f_P(\phi)+\bar{f}_P(\phi))d\epsilon\\ &=\int(\mathcal{T}_{P,L}+\mathcal{T}_{P,R})(f_L+f_R)d\epsilon,\end{aligned} \quad (47)$$

Given the linear relation between $\mathcal{T}_{L,P}$ and $\mathcal{T}_{R,P}$, this equality holds separately for each transmission function,

$$\begin{aligned}&\int\mathcal{T}_{P,\nu}(f_P(\phi)+\bar{f}_P(\phi))d\epsilon\\ &=\int\mathcal{T}_{P,\nu}(f_L+f_R)d\epsilon \quad \nu=L,R,\end{aligned} \quad (48)$$

providing $\mathcal{R} = 0$ in Eq. (23). Thus, if $\mathcal{T}_{P,L} = \mathcal{T}_{L,P} = \chi\mathcal{T}_{P,R}$, rectification is absent. In physical terms, the junction conducts symmetrically for forward and reversed direction, though many-body effects are presented, if we satisfy two conditions: (i) Spatial asymmetry is included in an energy-independent manner, for example using different broad-band hybridization parameters at the two ends. (ii) Time reversal symmetry is protected.

We now derive symmetry relations for left-right symmetric systems with broken time-reversal symmetry. In this case the mirror symmetry $\mathcal{T}_{P,L}(\phi) = \mathcal{T}_{P,R}(-\phi)$ applies, translating to

$$\mathcal{T}_{P,L}(\phi) = \mathcal{T}_{R,P}(\phi). \quad (49)$$

When used in Eq. (46), we note that the distributions should obey

$$\bar{f}_P(\phi) = f_P(-\phi), \quad (50)$$

leading to $\bar{\mu}_P(\phi) = \mu_P(-\phi)$. We emphasize that $\mu_P(\phi)$ itself does not posses a phase symmetry.

Since the leakage of charge into the probe is prohibited, the deviation from phase rigidity, Eq. (21), can be also expressed in terms of the current I_R, to provide (note the sign convention)

$$\begin{aligned}\Delta I(\phi) &= \frac{1}{2}\int d\epsilon[(\mathcal{T}_{L,R}-\mathcal{T}_{R,L})f_L\\ &- \mathcal{T}_{R,P}f_P(-\phi)+\mathcal{T}_{P,R}f_P(\phi)].\end{aligned} \quad (51)$$

We define ΔI by the average of Eqs. (21) and (51),

$$\begin{aligned}\Delta I(\phi) &= \frac{1}{4}\int d\epsilon\Big[(\mathcal{T}_{L,R}-\mathcal{T}_{R,L})(f_L+f_R)\\ &+ (\mathcal{T}_{L,P}-\mathcal{T}_{R,P})f_P(-\phi)+(\mathcal{T}_{P,R}-\mathcal{T}_{P,L})f_P(\phi)\Big].\end{aligned}$$

We proceed and make use of two relations: $\mathcal{T}_{L,R}-\mathcal{T}_{R,L} = \mathcal{T}_{P,L}-\mathcal{T}_{L,P}$. and Eq (49), valid in geometrically symmetric junctions. With this at hand we write

$$\begin{aligned}&\Delta I(\phi) = \frac{1}{4}\int(\mathcal{T}_{P,L}-\mathcal{T}_{P,R})(f_L+f_R-f_P(\phi)-\bar{f}_P(\phi))d\epsilon\\ &=\mathcal{R}(\phi) = -\mathcal{R}(-\phi),\end{aligned} \quad (52)$$

This concludes our derivation of the MF symmetries,

$$\Delta I(\phi) = \mathcal{R}(\phi) = -\mathcal{R}(-\phi), \quad \mathcal{D}(\phi) = \mathcal{D}(-\phi). \quad (53)$$

In spatially symmetric systems odd conductance terms acquire even symmetry with respect to the magnetic field, as noted experimentally[35,38], while even conductance terms, constructing $\mathcal{R}$, are odd with respect to ϕ. This result was also obtained analytically in a two-terminal AB interferometer, when strong electron-electron interactions were taken into account in the quantum dot, beyond the mean-field approach[44]. The relation $\Delta I(\phi) = \mathcal{R}(\phi)$ could be exploited in experimental studies: One could determine whether a quantum dot junction is L-R symmetric by testing this equality.

We now emphasize the following points: (i) Eq. (53) does not hold when a spatial asymmetry is introduced, by coupling the scattering centers unevenly to the leads. (ii) The derivation of Eq. (53) does not assume a particular form for the density of states of either the L and R leads, or the probe reservoir, as long as Eq. (49) is satisfied. (iii) The symmetry relations obtained here are valid under the more restrictive (non-dissipative) voltage-temperature probe, Eq. (12). (iv) The analysis in this section reveals sufficient conditions for charge rectification for structurally *symmetric* junctions: $\mathcal{R}(\phi) \neq 0$ when time-reversal symmetry is broken, $\phi \neq 2\pi n$, and inelastic scatterings are allowed. (v) In Appendix A we prove that the double-dot AB interferometer supports an extended version of the symmetry (53) when spatial asymmetries are introduced, see Eq. (A15).

VI. BEYOND LINEAR RESPONSE: SPATIALLY ASYMMETRIC SETUPS

We adopt a double-dot AB model, see Fig. 2, allow for inelastic effects and spatial asymmetries, and derive

magnetic field-gate voltage symmetry relations.

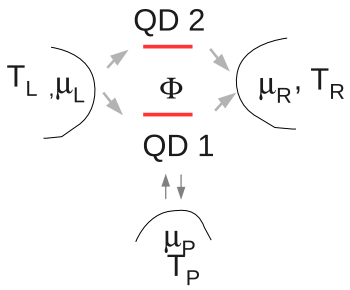

FIG. 2: Scheme of a double-dot AB interferometer susceptible to many-body effects. The two quantum dots (QD) are each represented by a single electronic level, which are not directly coupled. The total magnetic flux is denoted by Φ. Dot '1' may be susceptible to elastic dephasing and inelastic effects, introduced here through the coupling of this dot to a probe, the terminal P.

A. Model: Double-dot Interferometer

We focus on an AB setup with a quantum dot located at each arm of the interferometer. The dots are connected to two metal leads maintained in a biased state. The model consists of a probe, responsible of (effective) inelastic scattering of electrons on the dots. For simplicity, we do not consider electron-electron interactions and the Zeeman effect, thus, we can ignore the spin degree of freedom and describe each quantum dot by a spinless electronic level. The total Hamiltonian includes the following terms,

$$H = H_S + \sum_{\nu=L,R,P} H_\nu + \sum_{\nu=L,R} H_{S,\nu} + H_{S,P} \qquad (54)$$

The subsystem Hamiltonian includes two (uncoupled) electronic states

$$H_S = \sum_{n=1,2} \epsilon_n a_n^\dagger a_n. \qquad (55)$$

The three reservoirs (metals) comprise of a collection of non-interacting electrons,

$$H_\nu = \sum_{j\in\nu} \epsilon_j a_j^\dagger a_j. \qquad (56)$$

Here $a_j^\dagger$ (a_j) are fermionic creation (annihilation) operators of electrons with momentum j and energy ϵ_j. $a_n^\dagger$ and a_n are the respective operators for the dots. The subsystem-bath coupling terms are given by

$$\begin{aligned} H_{S,L} + H_{S,R} \;=\; & \sum_{n=1,2}\sum_{l\in L} v_{n,l} a_n^\dagger a_l e^{i\phi_n^L} \\ & + \sum_{n=1,2}\sum_{r\in R} v_{n,r} a_r^\dagger a_n e^{i\phi_n^R} + h.c.. \end{aligned}$$

For simplicity, we set only dot '1' to couple to the probe

$$H_{S,P} = \sum_{p\in P} v_{1,p} a_1^\dagger a_p + h.c. \qquad (57)$$

Here $v_{n,j}$ is the coupling strength of dot n to the j state of the J bath. Below we assume that this parameter does not depend on the $n = 1, 2$ level index. ϕ_n^L and ϕ_n^R are the AB phase factors, acquired by electron waves in a magnetic field perpendicular to the device plane. These phases are constrained to satisfy

$$\phi_1^L - \phi_2^L + \phi_1^R - \phi_2^R = \phi \qquad (58)$$

and we adopt the gauge $\phi_1^L - \phi_2^L = \phi_1^R - \phi_2^R = \phi/2$.

We voltage-bias the system, $\Delta\mu \equiv \mu_L - \mu_R$, with $\mu_{L,R}$ as the chemical potential of the metals, and use the convention that a positive current is flowing left-to-right. While we bias the system in a symmetric manner, $\mu_L = -\mu_R$, this choice does not limit the generality of our discussion since the dots may be gated away from the so called "symmetric point" at which $\mu_L - \epsilon_n = \epsilon_n - \mu_R$.

B. Green's function expressions

Our model does not include interacting particles, thus its steady-state characteristics can be written exactly using the nonequilibrium Green's function approach[56,57]. Transient effects were recently explored in Refs.[58,59]. Our recent study[60] details relevant derivations, thus we only include here the principal expressions. In terms of the Green's function, the transmission coefficient is defined as

$$\mathcal{T}_{\nu,\xi} = \mathrm{Tr}[\Gamma^\nu G^+ \Gamma^\xi G^-], \qquad (59)$$

where the trace is performed over the states of the subsystem (dots). In our model the matrix G^+ ($G^- = [G^+]^\dagger$) takes the form

$$G^+ = \begin{bmatrix} \epsilon - \epsilon_1 + \frac{i(\gamma_L+\gamma_R+\gamma_P)}{2} & \frac{i\gamma_L}{2}e^{i\phi/2} + \frac{i\gamma_R}{2}e^{-i\phi/2} \\ \frac{i\gamma_L}{2}e^{-i\phi/2} + \frac{i\gamma_R}{2}e^{i\phi/2} & \epsilon - \epsilon_2 + \frac{i(\gamma_L+\gamma_R)}{2} \end{bmatrix}^{-1},$$

with the hybridization matrices satisfying

$$\Gamma^L = \gamma_L \begin{bmatrix} 1 & e^{i\phi/2} \\ e^{-i\phi/2} & 1 \end{bmatrix}, \quad \Gamma^R = \gamma_R \begin{bmatrix} 1 & e^{-i\phi/2} \\ e^{i\phi/2} & 1 \end{bmatrix}$$
$$\Gamma^P = \gamma_P \begin{bmatrix} 1 & 0 \\ 0 & 0 \end{bmatrix} \qquad (60)$$

The coupling energy between the dots and leads is given by $\gamma_\nu(\epsilon) = 2\pi \sum_{j\in\nu} |v_j|^2 \delta(\epsilon - \epsilon_j)$. In the wide-band limit adopted in this work γ_ν are taken as energy independent parameters.

We now assume that the dots are energy-degenerate, $\epsilon_d \equiv \epsilon_1 = \epsilon_2$, but allow for a spatial asymmetry in the

form $\gamma_L \neq \gamma_R$. The transmission functions are given by

$$\begin{aligned}
\mathcal{T}_{L,R} &= \frac{\gamma_L\gamma_R}{\Delta(\epsilon,\phi)}\left[4(\epsilon-\epsilon_d)^2\cos^2\frac{\phi}{2}+\frac{\gamma_P^2}{4}+\gamma_P(\epsilon_d-\epsilon)\sin\phi\right]\\
\mathcal{T}_{L,P} &= \frac{\gamma_L\gamma_P}{\Delta(\epsilon,\phi)}\left[(\epsilon-\epsilon_d)^2+\gamma_R^2\sin^2\frac{\phi}{2}+\gamma_R(\epsilon-\epsilon_d)\sin\phi\right]\\
\mathcal{T}_{R,P} &= \frac{\gamma_R\gamma_P}{\Delta(\epsilon,\phi)}\left[(\epsilon-\epsilon_d)^2+\gamma_L^2\sin^2\frac{\phi}{2}-\gamma_L(\epsilon-\epsilon_d)\sin\phi\right]
\end{aligned} \tag{61}$$

with the denominator an even function of ϕ,

$$\begin{aligned}
\Delta(\epsilon,\phi) &= \left[(\epsilon-\epsilon_d)^2-\gamma_L\gamma_R\sin^2\frac{\phi}{2}-\frac{(\gamma_L+\gamma_R)\gamma_P}{4}\right]^2\\
&+ \left(\gamma_L+\gamma_R+\frac{\gamma_P}{2}\right)^2(\epsilon-\epsilon_d)^2.
\end{aligned} \tag{62}$$

It is trivial to confirm that in the absence of the probe, an even symmetry of the current with ϕ is satisfied, beyond linear response[61].

$$I_L(\phi) = \int d\epsilon \frac{4\gamma_L\gamma_R(\epsilon-\epsilon_d)^2\cos^2\frac{\phi}{2}[f_L(\epsilon)-f_R(\epsilon)]}{\left[(\epsilon-\epsilon_d)^2-\gamma_L\gamma_R\sin^2\frac{\phi}{2}\right]^2+(\gamma_L+\gamma_R)^2(\epsilon-\epsilon_d)^2}$$

With the probe, inspecting the transmission functions in conjunction with Eq. (38), we immediately conclude that under spatial asymmetries the probe chemical potential does not obey a particular symmetry, even in linear response when phase rigidity is trivially obeyed, see Sec. IV B.

We now discuss the properties of the probe when the interferometer is L-R symmetric, $\gamma/2 = \gamma_L = \gamma_R$. The transmission functions satisfy $\mathcal{T}_{R,P}(\epsilon,\phi) = \mathcal{T}_{P,L}(\epsilon,\phi)$. We substitute these expressions into Eq. (25) and resolve the dephasing probe distribution[60]

$$\begin{aligned}
f_P^D(\epsilon,\phi) &= \frac{f_L(\epsilon)+f_R(\epsilon)}{2}\\
&+ \frac{\gamma(\epsilon-\epsilon_d)\sin\phi}{4\left[(\epsilon-\epsilon_d)^2+\omega_0^2\right]}[f_L(\epsilon)-f_R(\epsilon)]
\end{aligned} \tag{63}$$

with $\omega_0 = \frac{\gamma}{2}\sin\frac{\phi}{2}$. The nonequilibrium term in this distribution is *odd* in the magnetic flux. Similarly, when a voltage probe (V) is implemented, analytic results can be obtained in the linear response regime,

$$\mu_P^V(\phi) = \Delta\mu\sin\phi\frac{\int d\epsilon\frac{\partial f_a}{\partial\epsilon}\frac{\gamma(\epsilon-\epsilon_d)}{\Delta(\epsilon,\phi)}}{\int d\epsilon\frac{\partial f_a}{\partial\epsilon}\frac{2(\epsilon-\epsilon_d)^2+\frac{1}{2}\gamma^2\sin^2\frac{\phi}{2}}{\Delta(\epsilon,\phi)}}. \tag{64}$$

Here f_a stands for the equilibrium (zero bias) Fermi-Dirac function. This chemical potential is an *odd* function of the magnetic flux, though phase rigidity is maintained in the linear response regime.

C. Generalized magnetic field-gate voltage symmetries

The MF symmetry relations (53) are not respected when the spatial mirror symmetry is broken. Instead, in Appendix A we prove that in a generic model for a double-dot interferometer susceptible to inelastic effects the following result holds

$$\mathcal{R} = -\mathcal{C}(\mathcal{R}), \quad \mathcal{D} = \mathcal{C}(\mathcal{D}). \tag{65}$$

Here $\mathcal{C}$ stands for the charge conjugation operator, transforming electrons to holes and vise versa. In terms of the parameters of our AB interferometer model, this relation reduces to the following magnetic flux-gate voltage (MFGV) symmetries,

$$\begin{aligned}
\mathcal{R}(\epsilon_d,\phi) &= -\mathcal{R}(-\epsilon_d,-\phi),\\
\mathcal{D}(\epsilon_d,\phi) &= \mathcal{D}(-\epsilon_d,-\phi).
\end{aligned} \tag{66}$$

Since the energies of the dots can be modulated with a gate voltage[40], these generalized symmetries can be examined experimentally.

We also point out that it can be immediately confirmed that under the mirror symmetry operation $\gamma_L \leftrightarrow \gamma_R$ and $\phi \to -\phi$ the following symmetry holds,

$$\begin{aligned}
\mathcal{R}(\gamma_L,\gamma_R,\phi) &= -\mathcal{R}(\gamma_R,\gamma_L,-\phi),\\
\mathcal{D}(\gamma_L,\gamma_R,\phi) &= \mathcal{D}(\gamma_R,\gamma_L,-\phi).
\end{aligned} \tag{67}$$

For details see Appendix A.

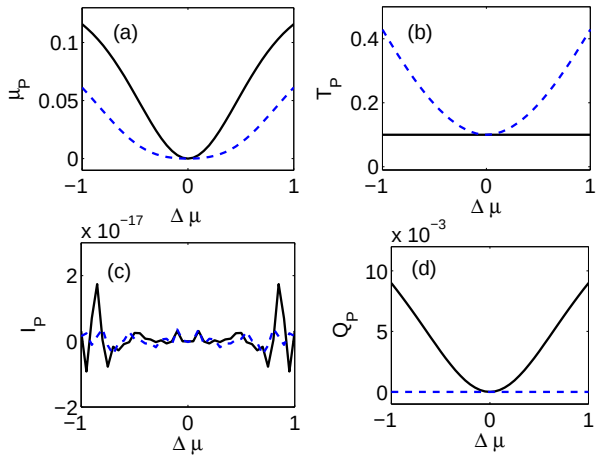

FIG. 3: Self-consistent parameters of the voltage probe (full) and the voltage-temperature probe (dashed), displaying disparate behavior far from equilibrium: (a) Probe chemical potential, (b) temperature. We also show (c) the magnitude of net charge current from the probe and (d) net heat current from the conductor towards the probe. The interferometer consists two degenerate levels with $\epsilon_{1,2} = 0.15$ coupled evenly to the metal leads $\gamma_{L,R} = 0.05$. Other parameters are $\gamma_P = 0.1$, $\phi = 0$, and $T_L = T_R = 0.1$. The probe temperature is set at $T_P = 0.1$ in the calculations of the voltage probe.

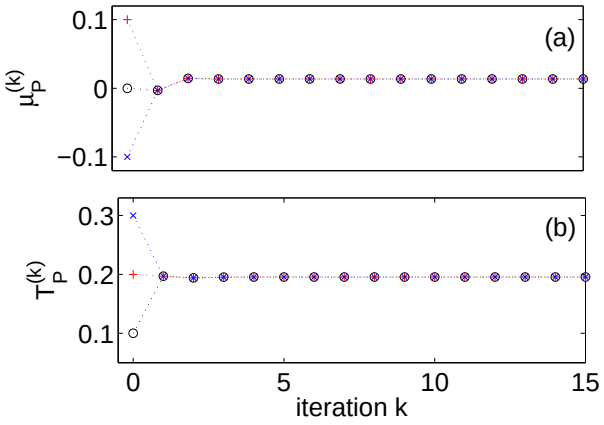

FIG. 4: Insensitivity of the parameters of the voltage-temperature probe [Eq. (13)] to initial conditions. (a) chemical potential of the probe and (b) its temperature. The different initial conditions are identified by the values at the first iteration. The interferometer's parameters follow Fig. 3 with $\Delta\mu = 0.5$ and $T_L = T_R = 0.1$.

VII. NUMERICAL SIMULATIONS

Using numerical simulations we demonstrate the behavior of the voltage and the voltage-temperature probes far from equilibrium, and the implications on phase rigidity and magnetic field symmetries.

A. Probe parameters

We consider the model Eq. (54) and implement inelastic effects with the dissipative voltage probe, by solving the probe condition (8) numerically-iteratively, using Eq. (9), to obtain μ_P. We also investigate the transport behavior of the model under the more restrictive dissipationless voltage-temperature probe, by solving Eq. (13) to obtain both μ_P and T_P.

Fig. 3 displays the self-consistent probe parameters μ_P and T_P for $\phi = 0$ when heat dissipation is allowed at the probe (full line), and when neither heat dissipation nor charge leakage take place within P (dashed line). We find that the probe parameters largely vary depending on the probe condition, particularly at high biases when significant heat dissipation can take place [panel (d)]. We also verify that when Newton-Raphson iterations converge, the charge current to the probe is negligible, $|I_P/I_L| < 10^{-12}$. Similarly, the heat current in the voltage-temperature probe is negligible once convergence is reached.

Uniqueness of the parameters of the voltage and temperature probes has been recently proved in Ref.[15]. We complement this analytical analysis and demonstrate that the parameters of the voltage-temperature probe are insensitive to the initial conditions adopted, see Fig. 4. Convergence has been typically achieved with ~ 5 iterations. While the voltage probe had easily converged even at large biases, we could not manage to converge the voltage-temperature probe parameters at large biases $\Delta\mu > 1$ and low temperatures $T_{L,R} < 1/50$ since eliminating heat dissipation within the probe requires extreme values, leading to numerical divergences within the model parameters adopted.

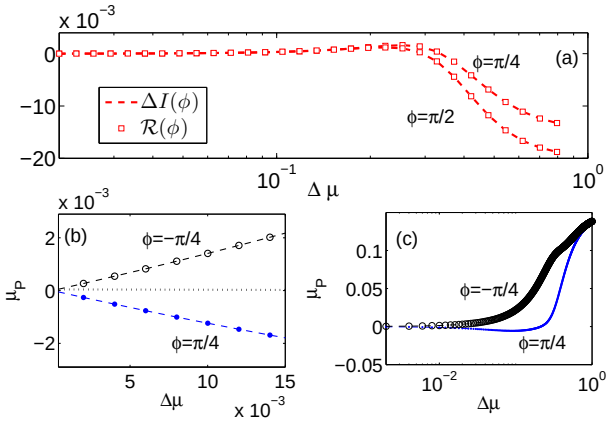

FIG. 5: (a) MF symmetry and rectification in spatially symmetric junctions. (b) Chemical potential of the probe in the linear response regime. (c) Chemical potential of the probe beyond linear response. The junction's parameters are $\epsilon_1 = \epsilon_2 = 0.15$, $\gamma_P = 0.1$, $\beta_a = 50$ and $\gamma_L = \gamma_R = 0.05$.

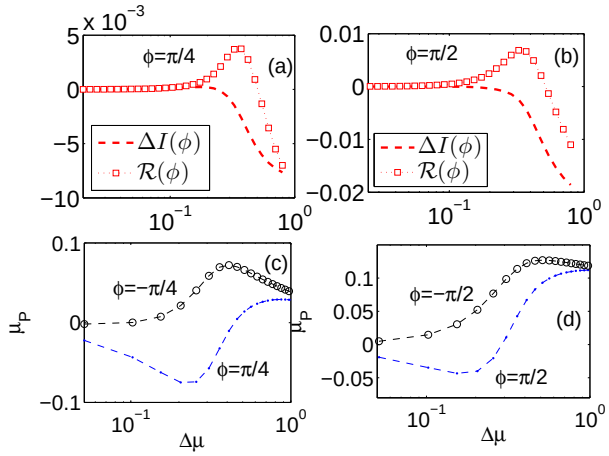

FIG. 6: Breakdown of the MF symmetry relations for spatially asymmetric junctions, $\gamma_L = 0.05 \neq \gamma_R = 0.2$. (a)-(b) ΔI (dashed) and $\mathcal{R}$ (square) for $\phi = \pi/4$ and $\pi/2$. The corresponding probe potential is displayed in panel (c) for $\phi = \pm\pi/4$ and in panel (d) for $\phi = \pm\pi/2$. Other parameters are $\epsilon_1 = \epsilon_2 = 0.15$, $\gamma_P = 0.1$ and $\beta_a = 50$.

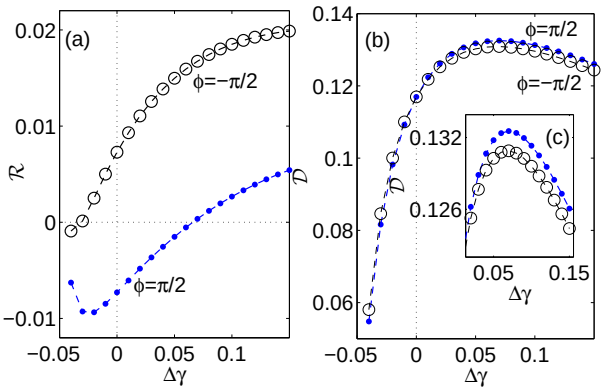

FIG. 7: (a)-(b) Even $\mathcal{R}$ and odd $\mathcal{D}$ conductance coefficients as a function of the coupling asymmetry $\Delta\gamma = \gamma_R - \gamma_L$ with $\gamma_L = 0.05$. (c) Zoom over $\mathcal{D}$. Other parameters are $\epsilon_1 = \epsilon_2 = 0.15$, $\gamma_P = 0.1$, $\Delta\mu = 0.4$ and $\beta_a = 50$.

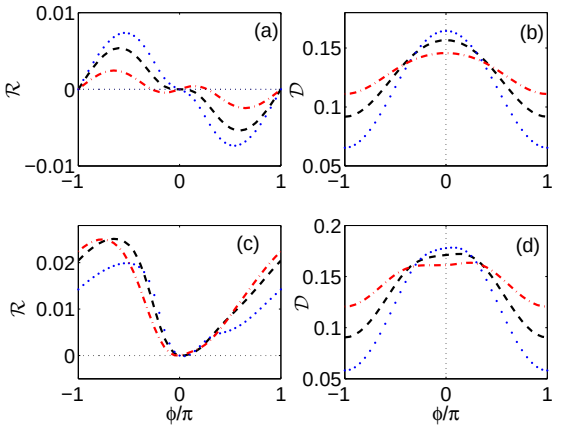

FIG. 8: Effect of the voltage probe hybridization strength on even ($\mathcal{R}$) and odd ($\mathcal{D}$) conductance terms. (a)-(b) Spatially symmetric system, $\gamma_L = \gamma_R = 0.05$. (c)-(d) Spatially asymmetric junction, $\gamma_L = 0.05 \neq \gamma_R = 0.2$. $\gamma_P = 0.1$ (dot), $\gamma_P = 0.2$ (dashed line) and $\gamma_P = 0.4$ (dashed-dotted). Light dotted lines represent symmetry lines. Other parameters are $\Delta\mu = 0.4$, $\epsilon_1 = \epsilon_2 = 0.15$, $\beta_a = 50$.

B. Nonlinear transport with dissipative inelastic effects

In this subsection we examine the nonlinear transport behavior of an AB interferometer coupled to a voltage probe. In Fig. 5 (a) we display the measure ΔI as a function of bias for a spatially symmetric system using two representative phases, $\phi = \pi/2$ and $\pi/4$. We confirm numerically that in the linear response regime $\Delta I = 0$. More generally, the relation $\Delta I = \mathcal{R}$ is satisfied for all biases, as expected from Eq. (53). Our conclusions are intact when an "up-down" asymmetry is implemented in the form $\epsilon_1 \neq \epsilon_2$[50]. The corresponding chemical potential of the probe is shown in Fig. 5(b)-(c) for $\phi = \pi/4$. In the linear response regime it grows linearly with $\Delta\mu$ and it obeys an odd symmetry relation, $\mu_P(\phi) = -\mu_P(-\phi)$. Beyond linear response μ_P does not follow neither an even nor an odd phase symmetry, but at large enough biases it is independent of the sign of the phase.

Fig. 6 displays results when spatial asymmetry in the form $\gamma_L \neq \gamma_R$ is implemented. Here we observe that $\Delta I \neq \mathcal{R}$, and that the probe chemical potential does not satisfy an odd symmetry with the magnetic phase, even in the linear response regime.

As the breakdown of the MF symmetries (53) occurs under a spatial asymmetry in the presence of inelastic effects, we study next the role of γ_P, $\Delta\gamma \equiv \gamma_R - \gamma_L$ and the metals temperature β_a^{-1} on these relations.

In Fig. 7 (a)-(b) we extract $\mathcal{D}$, and present it along with $\mathcal{R}$ as a function of $\Delta\gamma$ We note that the symmetry of $\mathcal{R}$ is feasibly broken with small spatial asymmetry, while $\mathcal{D}$ is more robust. The role of the coupling strength γ_P is considered in Fig. 8. First, in spatially symmetric systems we confirm again that the MF relations (53) are satisfied, and we note that as γ_P increases, the variation of $\mathcal{D}$ and $\mathcal{R}$ with phase is fading out. Quite interestingly, the rectification contribution $\mathcal{R}$ may flip sign with γ_P, for

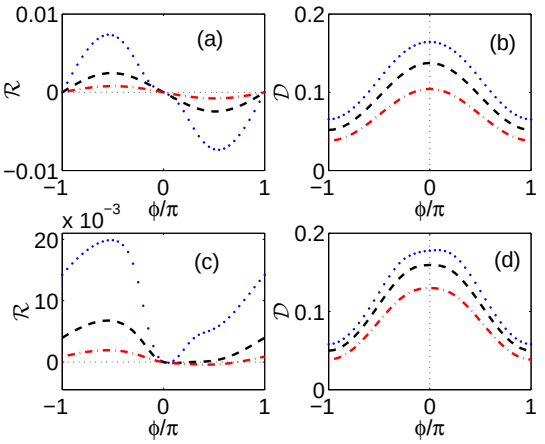

FIG. 9: Temperature dependence of even and odd conductance terms. (a)-(b) Spatially symmetric system, $\gamma_L = \gamma_R = 0.05$. (c)-(d) Spatially asymmetric system, $\gamma_L = 0.05 \neq \gamma_R = 0.2$. In all panels $\beta_a = 50$ (dots), $\beta_a = 10$ (dashed line) and $\beta_a = 5$ (dashed-dotted line). The light dotted lines mark symmetry lines. Other parameters are $\Delta\mu = 0.4$, $\gamma_P = 0.1$ and $\epsilon_1 = \epsilon_2 = 0.15$.

a range of phases. (The sign of $\mathcal{R}$ reflects whether the total current has a larger magnitude in the forward or backward bias polarity). Second, when a spatial asymmetry is introduced we note a strong breakdown of the MF phase symmetry for $\mathcal{R}$, while the coefficient $\mathcal{D}$ still closely follows the MF symmetry[35]. Interestingly, with increasing γ_P the variation of $\mathcal{D}$ with phase is washed out (panel d), but even conductance terms show a stronger alteration with ϕ (panel c). Thus, even and odd conductance terms respond distinctively to decoherring and

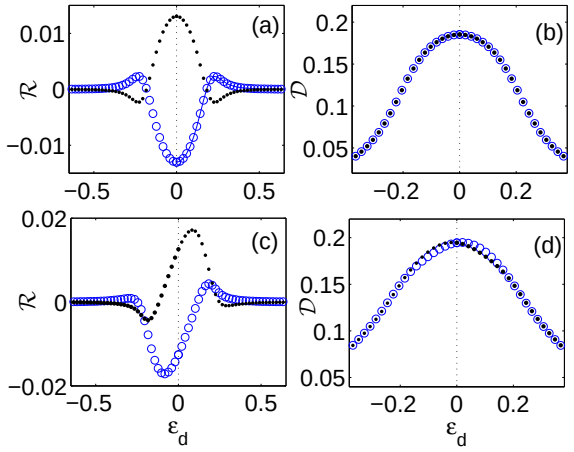

FIG. 10: Magnetic field- gate voltage (MFGV) symmetries. (a)-(b) Even and odd conductance terms for a spatially symmetric junction with $\gamma_L = \gamma_R = 0.05$. (c)-(d) Even and odd conductance terms for a spatially asymmetric system with $\gamma_L = 0.05$, $\gamma_R = 0.2$, demonstrating that $\mathcal{R}(\epsilon_d, \phi) = -\mathcal{R}(-\epsilon_d, -\phi)$, $\mathcal{D}(\epsilon_d, \phi) = \mathcal{D}(-\epsilon_d, -\phi)$. In all cases $\phi = -\pi/4$ (small dots) and $\phi = \pi/4$ (empty circle), $\Delta\mu = 0.4$, $\gamma_P = 0.1$ and $\beta_a = 50$.

inelastic processes.

In Fig. 9 we consider the role of the reservoirs temperatures on the conductance coefficients. With increasing temperature a monotonic erosion of the amplitude of all conductance terms with phase takes place. This should be contrasted to the non-monotonic role of γ_P on $\mathcal{R}$, as exposed in Fig. 8.

Inspecting e.g., Fig. 9 we point out that in our construction $\mathcal{R}(\phi = 0) = 0$, even in the presence of geometrical asymmetry, see discussion following Eq. (48). We recall that many-body effects are presented here effectively, thus this observation is not trivial given the common expectation that the combination of many-body interactions and spatial asymmetry should bring in the current rectification effect[47]. Indeed, extended models in which the system is connected to the reservoirs indirectly, through "linker" states, present rectification even at zero magnetic field, as long as both spatial asymmetry and inelastic effects are introduced[13].

The scan of the current with $\epsilon_d = \epsilon_{1,2}$ is presented in Fig. 10. When $\epsilon_d > \Delta\mu$, Onsager symmetry is practically respected since the linear response limit is practiced, providing $\Delta I \sim \mathcal{R} \sim 0$. More significantly, this figure reveals the MFGV symmetry (66), valid irrespective of spatial asymmetries and many-body (inelastic) effects. This symmetry immediately implies that at the so-called "symmetric point", when $\epsilon_d = 0$ (set at the Fermi energy), $\mathcal{R}(\phi)$ is an odd function of the magnetic flux irrespective of spatial asymmetries. This behavior is displayed in Fig. 11. We also note that at the symmetric point the probe chemical potential is identically zero (Fermi energy) in symmetric setups, and it satisfies $\mu_P(\phi) = \mu_P(-\phi)$ far from equilibrium for setups with a broken inversion symmetry, see Fig. 12.

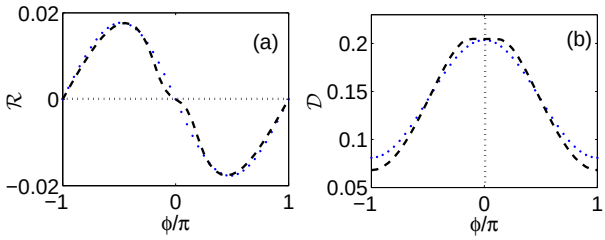

FIG. 11: MF symmetries at the symmetric point $\epsilon_d = \epsilon_1 = \epsilon_2 = 0$. (a) Even $\mathcal{R}$ (b) odd $\mathcal{D}$ conductance terms for spatially symmetric $\gamma_L = \gamma_R = 0.05$ (dots) and asymmetric situations $\gamma_L = 0.05$, $\gamma_R = 0.2$ (dashed lines). Other parameters are $\Delta\mu = 0.4$, $\gamma_P = 0.1$ and $\beta_a = 50$.

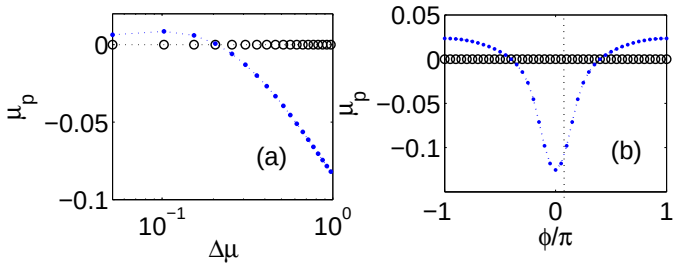

FIG. 12: (a)-(b) Chemical potential of the probe at the symmetric point, for spatially symmetric $\gamma_L = \gamma_R = 0.05$ (circles), and asymmetric $\gamma_L = 0.05 \neq \gamma_R = 0.2$ cases (dots). (a) Bias dependence of μ_P. The lines contain the overlapping $\phi = \pm\pi/4$ results. (b) Magnetic flux dependency of μ_P for $\Delta\mu = 0.4$. Other parameters are $\beta_a = 50$ and $\gamma_P = 0.1$.

C. Nonlinear transport with non-dissipative inelastic effects

The simulations presented throughout Figs. 5-12 were obtained under the voltage probe condition, thus heat dissipation takes place at the probe. In Fig. 13 we show that the breakup of the MF symmetries occurs in spatially asymmetric setups under the more restrictive voltage-temperature probe, when only *non-dissipative* inelastic effects are allowed. We again note that the breakdown of the phase symmetry of $\mathcal{D}$ is small, one order of magnitude below the variation in $\mathcal{R}$.

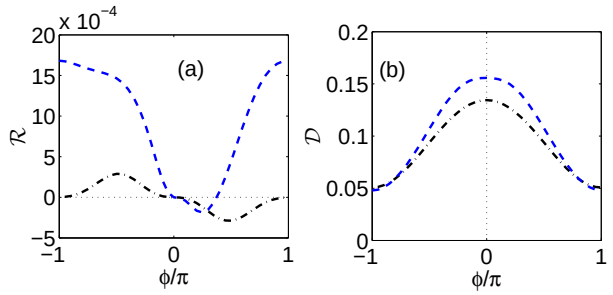

FIG. 13: Voltage-temperature probe. (a) $\mathcal{R}$ and (b) $\mathcal{D}$ in spatially symmetric case (dashed-dotted lines) $\gamma_{L,R} = 0.05$ and asymmetric setups (dashed lines) $\gamma_L = 0.05 \neq \gamma_R = 0.2$. $\beta_a = 10$, $\gamma_P = 0.1$, $\epsilon_{1,2} = 0.15$.

D. Relation of results to other treatments

Magnetic field symmetries of nonlinear transport were analyzed in several other papers by including electron-electron interactions at different levels: mean field, Coulomb blockage, Kondo limit[41–44]. Particularly, in Ref.[41] and more recent studies[72] electron-electron interactions are taken into account by considering the nonlinear response of the electronic potential landscape in the conductor to the applied voltage. This is done by adopting scattering theory: The argument is that in a nonequilibrium situation the charge density in the conductor piles up in response to the applied voltage. The scattering matrix then becomes bias dependent through its dependence on the potential landscape in the conductor. Nonlinear conductance terms contain information about charge response in the system, effects that are non-even in the magnetic field, and this leads to deviations from Onsager's reciprocity relation beyond linear response.

In our approach, we include interaction effects in the interior of the conductor within an alternative mean, the probe. We recall that this tool emulates (electron-electron, electron-phonon) interactions in the conductor as follows: First, we apply a bias and set the temperatures at the two boundaries, μ_ν, β_ν. We then include many-body effects at the conductor, e.g., inelastic effects, using a voltage probe, by demanding that the charge current towards it vanishes. This constraint sets the probe parameters μ_P and β_P, describing charge distribution at the interior of the device. With these statistical measures, chemical potentials and temperatures, we can calculate the charge current in the Landauer picture.

Our calculations provide us with the self-consistent probe chemical potential, and this measure is generally neither even nor odd in the magnetic field, even in linear response. Fig. 6 indeed shows that μ_P depends on the applied bias and the magnetic flux, generally missing magnetic field symmetries. We can interpret the probe potential as the local-internal potential in the conductor. We highlight that in our approach we do not set it by hand. Rather, by setting boundary conditions for the L and R terminals, and by imposing the probe constraint, we receive the probe potential as a self-consistent solution.

We now argue that our analysis here, based on the probe technique, has a comparable status to to the treatment of Ref.[41], and related studies, which are based on the behavior of the screening potential under bias. The screening potential is a *macroscopic, electrostatics-theory* property which responds to interactions between microscopic degrees of freedom. Similarly, the probe potential is an effective *statistical* measure, describing the internal potential, enclosing effects of microscopic scattering processes in the conductor. Both the screening potential and the probe potential develop from genuine many-body effects, and while these measures are not necessarily equivalent, they both consistently incorporate effects beyond linear response: The screening potential is written as an expansion in voltage, the probe potential is determined self consistently, at arbitrarily large applied voltage.

We conclude this discussion by emphasizing that the derivation of symmetries beyond linear response should be eventually done beyond phenomenological approaches and mean field treatments, by adopting model Hamiltonians with genuine many-body interactions[44], and by using exact quantum techniques[62].

VIII. SUMMARY

We have studied the role of elastic and inelastic scattering effects on magnetic field symmetries of nonlinear conductance terms using Büttiker's probe technique. For spatially symmetric junctions we proved the validity of the MF symmetries for charge transport $\mathcal{D}(\phi) = \mathcal{D}(-\phi)$ and $\mathcal{R}(\phi) = -\mathcal{R}(-\phi)$, though many-body inelastic effects, introduced via the probe, are asymmetric in magnetic flux. We demonstrated the breakdown of these MF symmetries when the junction has a left-right asymmetry, in the presence of inelastic effects. Using a double-dot AB interferometer model we showed that it respects more general MFGV symmetry relations, $\mathcal{R}(\epsilon_d, \phi) = -\mathcal{R}(-\epsilon_d, -\phi)$ and $\mathcal{D}(\epsilon_d, \phi) = \mathcal{D}(-\epsilon_d, -\phi)$.

We now recall that these sets of symmetries were derived only based on the symmetry of the probe distribution function f_P, upon reversal of the applied bias. Considering a conductor coupled to a voltage probe and placed under both an applied temperature bias and a voltage bias, we write the formal expansion $I_L = -I_R = \sum_{n,m} G_{n,m} \Delta\mu^n \Delta T^m$ and identify $\mathcal{R} = \sum_{n+m=2k} G_{n,m} \Delta\mu^n \Delta T^m$, to contain even conductance terms, and the complementing term $\mathcal{D} = \sum_{n+m\neq 2k} G_{n,m} \Delta\mu^n \Delta T^m$. Following the discussion of Secs. V-VI, we can immediately confirm the validity of the MF and the MFGV symmetries implying that e.g. $G_{1,1}(\phi) = -G_{1,1}(-\phi)$ for spatially symmetric setups.

The model system investigated in Secs.VI-VII, the double-dot AB interferometer, offers a feasible setup for

devising rectifiers based on broken time reversal symmetry: We found that $\mathcal{R} \neq 0$, when two conditions are simultaneously met: (i) the magnetic flux obeys $\phi \neq 2\pi n$, n is an integer, (ii) and the probe introduces inelastic effects. However, when time reversal symmetry is maintained (when the flux obeys $\phi = 2n\pi$) our model does not bring about the rectification effect, even if the spatial mirror symmetry is broken. The technical reason is that in our minimal construction both dots are coupled to the L and R metals directly, with an energy independent hybridization constant. In extended models when the ring is coupled indirectly to the L and R metals, through a spacer state, geometrical rectification may develop even in the absence of the threading magnetic flux.

It is of interest to verify the results of this work by adopting a microscopic model with genuine many-body interactions[63–65], by modeling a quantum point contact[66,67] or an equilibrated phonon bath, exchanging energy with the junction's electronic degrees of freedom. This could be done by extending numerical and analytic studies, e.g., Refs.[68–70], to the nonlinear regime. It is also of interest to obtain the MF and the MFGV symmetries using a full-counting statistics approach[27,71].

We conclude this work by highlighting potential applications of the probe technique to far-from-equilibrium situations. In the linear response regime this self-consistent tool has been proven extremely useful for investigating the ballistic to diffusive crossover in electron[5,21] and phonon transport[23–25]. While explicit analytic results are missing beyond linear response, we have demonstrated here that one could still adopt this approach far from equilibrium and infer general transport symmetries, by analyzing the properties of the probe. Our simulations confirm the stability of the self-consistent numerical approach to far-from-equilibrium scenarios, and its utility for exploring transport properties. As this technique is no longer limited to the linear response limit or to weak (probe-conductor) coupling problems, it is now possible to explore its predictions (e.g., the rectification behavior) alongside quantum master equation approaches and other treatments incorporating genuine elastic dephasing and inelastic effects. Future studies will be devoted to the analysis of the thermoelectric effect under broken time reversal symmetry[8–10,70,72–74] in the far-from-equilibrium regime, and to the study of quantum transport, far from equilibrium, in networks with broken time reversal symmetry[75].

Acknowledgments

DS acknowledges support from the Natural Science and Engineering Research Council of Canada. The work of SB has been supported by the Early Research Award of DS. MB acknowledges financial support of IIT Bhubaneswar through seed money project SP0045. The authors acknowledge R. Härtle for useful comments.

Appendix A: Charge conjugation symmetries for a double-dot AB interferometer

We derive the MFGV symmetry relations by considering a double-dot interferometer model which does not necessarily acquire a spatial symmetry. Given the Hamiltonian (54)-(57), we introduce a charge conjugation operator $\mathcal{C}$ that acts to replace an electron by a hole[76],

$$\begin{aligned} \mathcal{C}(\epsilon_d) &= -\epsilon_d, \quad \mathcal{C}(\epsilon_k) = -\epsilon_k, \\ \mathcal{C}(v_{n,j}e^{i\phi_n}) &= -v^*_{n,j}e^{-i\phi_n}, \quad \mathcal{C}(\langle a^\dagger a\rangle) = 1 - \langle a^\dagger a\rangle. \end{aligned} \tag{A1}$$

Here $a^\dagger$ and a are fermionic creation and annihilation operators, respectively. Note that in our model the transmission function satisfies $\mathcal{T}(\epsilon, \epsilon_d, \phi) = \mathcal{T}(-\epsilon, -\epsilon_d, -\phi)$, i.e. it is invariant under charge conjugation. First, we need to find what symmetries does the probe chemical potential obey. Our derivation below relies on the following identity for the Fermi function,

$$\begin{aligned} f_\nu(-\epsilon, \mu_\nu) &= [e^{\beta(-\epsilon-\mu_\nu)} + 1]^{-1} \\ &= 1 - f_\nu(\epsilon, -\mu_\nu). \end{aligned} \tag{A2}$$

Since we use the convention $\mu_L = -\mu_R$, we conclude that $f_L(-\epsilon, \mu_L) = 1 - f_R(\epsilon, \mu_R)$. Next we omit the direct reference to the energy ϵ within $\mathcal{T}$ and the Fermi functions. Also, we do not write the phase ϕ in the transmission function, unless necessary to eliminate confusion.

We now study the probe condition (46) as is, under reversed bias voltage, and under charge conjugation,

$$\int d\epsilon(\mathcal{T}_{P,L} + \mathcal{T}_{P,R}) f_P(\mu_P(\epsilon_d, \phi, \mu_L, \mu_R)) = \int d\epsilon(\mathcal{T}_{L,P} f_L + \mathcal{T}_{R,P} f_R) \tag{A3}$$

$$\int d\epsilon(\mathcal{T}_{P,L} + \mathcal{T}_{P,R}) f_P(\mu_P(\epsilon_d, \phi, \mu_R, \mu_L)) = \int d\epsilon\left(\mathcal{T}_{L,P} f_R + \mathcal{T}_{R,P} f_L\right). \tag{A4}$$

$$\int d\epsilon(\mathcal{T}_{P,L} + \mathcal{T}_{P,R})[1 - f_P(-\mu_P(-\epsilon_d, -\phi, \mu_L, \mu_R))] = \int d\epsilon(\mathcal{T}_{L,P}[1 - f_R] + \mathcal{T}_{R,P}[1 - f_L]) \tag{A5}$$

For clarity, we explicitly noted the dependence of f_P on the chemical potential μ_P, itself obtained given the set of

parameters ϵ_d, ϕ, and $\mu_{L,R}$. Equation (A5) now reduces to

$$\int d\epsilon(\mathcal{T}_{P,L}+\mathcal{T}_{P,R})f_P(-\mu_P(-\epsilon_d,-\phi,\mu_L,\mu_R)) = \int d\epsilon(\mathcal{T}_{L,P}f_R+\mathcal{T}_{R,P}f_L). \quad \text{(A6)}$$

Comparing it to Eq. (A4) we immediately note that

$$f_P(-\mu_P(-\epsilon_d,-\phi,\mu_L,\mu_R)) = f_P(\mu_P(\epsilon_d,\phi,\mu_R,\mu_L). \quad \text{(A7)}$$

This result should be compared to Eq. (50), valid for spatially symmetric systems. Since the three reservoirs L, R, P are maintained at the temperature T_a, this relation implies that

$$\mu_P(\epsilon_d,\phi,\mu_L,\mu_R) = -\mu_P(-\epsilon_d,-\phi,\mu_R,\mu_L). \quad \text{(A8)}$$

We now utilize Eq. (A7) and derive symmetry relations for $\mathcal{R}$ and $\mathcal{D}$. We recall the explicit expressions for these measures, see the definitions (22) and (24) in Sec. III,

$$\begin{aligned}\mathcal{R} &= \frac{1}{2}\int d\epsilon\mathcal{T}_{P,L}\left[f_L+f_R-f_P(\mu_P(\epsilon_d,\phi,\mu_L,\mu_R))-f_P(\mu_P(\epsilon_d,\phi,\mu_R,\mu_L))\right]\\ \mathcal{D} &= \frac{1}{2}\int d\epsilon\Big\{(\mathcal{T}_{L,R}+\mathcal{T}_{L,P}+\mathcal{T}_{R,L})(f_L-f_R)-\mathcal{T}_{P,L}\left[f_P(\mu_P(\epsilon_d,\phi,\mu_L,\mu_R))-f_P(\mu_P(\epsilon_d,\phi,\mu_R,\mu_L)\right]\Big\} \quad \text{(A9)}\end{aligned}$$

The charge-conjugated expressions satisfy

$$\begin{aligned}\mathcal{C}(\mathcal{R}) &= \frac{1}{2}\int d\epsilon\mathcal{T}_{P,L}\left\{[1-f_R]+[1-f_L]-[1-f_P(-\mu_P(-\epsilon_d,-\phi,\mu_L,\mu_R))]-[1-f_P(-\mu_P(-\epsilon_d,-\phi,\mu_R,\mu_L)]\right\}\\ &= -\frac{1}{2}\int d\epsilon\mathcal{T}_{P,L}\left\{f_R+f_L-f_P(-\mu_P(-\epsilon_d,-\phi,\mu_L,\mu_R))-f_P(-\mu_P(-\epsilon_d,-\phi,\mu_R,\mu_L))\right\}\\ &= -\mathcal{R} \quad \text{(A10)}\end{aligned}$$

The last equality is reached by using Eq. (A7). Similarly, we obtain the symmetry of odd conductance terms as

$$\begin{aligned}\mathcal{C}(\mathcal{D}) &= \frac{1}{2}\int d\epsilon\Big\{(\mathcal{T}_{L,R}+\mathcal{T}_{L,P}+\mathcal{T}_{R,L})(1-f_R-1+f_L)\\ &- \mathcal{T}_{P,L}\left[1-f_P(-\mu_P(-\epsilon_d,-\phi,\mu_L,\mu_R))-1+f_P(-\mu_P(-\epsilon_d,-\phi,\mu_R,\mu_L))\right]\Big\}\\ &= \frac{1}{2}\int d\epsilon\Big\{(\mathcal{T}_{L,R}+\mathcal{T}_{L,P}+\mathcal{T}_{R,L})(f_L-f_R)+\mathcal{T}_{P,L}\left[f_P(-\mu_P(-\epsilon_d,-\phi,\mu_L,\mu_R))-f_P(-\mu_P(-\epsilon_d,-\phi,\mu_R,\mu_L))\right]\Big\}\\ &= \mathcal{D} \quad \text{(A11)}\end{aligned}$$

In the double-dot interferometer model these relations translate to the MFGV symmetries,

$$\begin{aligned}\mathcal{R}(\epsilon_d,\phi) &= -\mathcal{R}(-\epsilon_d,-\phi),\\ \mathcal{D}(\epsilon_d,\phi) &= \mathcal{D}(-\epsilon_d,-\phi). \quad \text{(A12)}\end{aligned}$$

In words, these relations point that even conductance terms flip sign when the magnetic flux is reversed and the gate is applied such that the dot energies ϵ_d switch position with respect to the equilibrium Fermi energy. Odd conductance terms are invariant under this transformation. For compactness, the derivation above has been performed assuming $\epsilon_d = \epsilon_1 = \epsilon_2$. It is trivial to extend our results beyond degeneracy.

We can also define the mirror symmetry operator $\mathcal{S}$. It interchanges the couplings, $\gamma_L \leftrightarrow \gamma_R$, and flips the phase $\phi \to -\phi$. In the double-dot interferometer the following relations are satisfied when we $\mathcal{S}$-operate the transmissions,

$$\begin{aligned}\mathcal{S}(\mathcal{T}_{L,R}(\epsilon,\phi)) &= \mathcal{T}_{R,L}(\epsilon,\phi),\\ \mathcal{S}(\mathcal{T}_{L,P}(\epsilon,\phi)) &= \mathcal{T}_{R,P}(\epsilon,\phi) \quad \text{(A13)}\end{aligned}$$

We can readily confirm from Eq. (46) that $\mathcal{S}(f_P) = \bar{f}_P$. Applying the mirror symmetry operator $\mathcal{S}$ on Eq. (A9)

we immediately reach the symmetry relations

$$\mathcal{S}(\mathcal{R}) = -\mathcal{R}, \quad \mathcal{S}(\mathcal{D}) = \mathcal{D} \tag{A14}$$

or explicitly,

$$\begin{aligned} \mathcal{R}(\gamma_R, \gamma_L, -\phi) &= -\mathcal{R}(\gamma_L, \gamma_R, \phi) \\ \mathcal{D}(\gamma_R, \gamma_L, -\phi) &= \mathcal{D}(\gamma_L, \gamma_R, \phi). \end{aligned} \tag{A15}$$

These relations generalize Eq. (53) to spatial asymmetric situations. Our numerical simulations reproduce these symmetries (not shown).

Appendix B: MF symmetries of nonlinear heat transport

In this Appendix we study symmetry relations of the electronic heat current under nonzero magnetic flux and a temperature bias $T_L \neq T_R$, in the absence of a potential bias, $\mu_a = \mu_L = \mu_R = \mu_P$. Using the temperature probe (10), we demand that heat dissipation at the probe diminishes, $Q_P = 0$, but allow for charge leakage in the probe. We now express the L to R heat current $Q_{\Delta T} \equiv Q_L = -Q_R$ in powers of the temperature bias as

$$Q_{\Delta T}(\phi) = K_1(\phi)\Delta T + K_2(\phi)(\Delta T)^2 + K_3(\phi)(\Delta T)^3 + ..., \tag{B1}$$

where $K_{n>1}$ are the nonlinear conductance coefficients. These coefficients depend on the junction parameters: energy, hybridization and possibly the temperature $T_a = (T_L + T_R)/2$. We define next symmetry measures for the heat current $Q_{\Delta T}$, parallel to Eqs. (16)-(24). First, we collect even conductance terms into $\mathcal{R}_{\Delta T}$,

$$\begin{aligned} &\mathcal{R}_{\Delta T}(\phi) \equiv \frac{1}{2}[Q(\phi) + \bar{Q}(\phi)] \\ &= K_2(\phi)(\Delta T)^2 + K_4(\phi)(\Delta T)^4 + ... \\ &= \int \frac{\mathcal{T}_{P,L} - \mathcal{T}_{P,R}}{4}(f_L + f_R - f_P(\phi) - \bar{f}_P(\phi))(\epsilon - \mu_a)d\epsilon \end{aligned} \tag{B2}$$

Here $\bar{Q}$ is defined as the heat current obtained upon interchanging the temperatures of the L and R terminals. We also study the behavior of odd conductance terms,

$$\mathcal{D}_{\Delta T}(\phi) \equiv K_1(\phi)\Delta T + K_3(\phi)(\Delta T)^3 + ... \tag{B3}$$

In the absence of the probe and in the linear response limit the heat current satisfies an even phase symmetry, $Q_{\Delta T}(\phi) = Q_{\Delta T}(-\phi)$. Deviations from this symmetry are collected into the measure

$$\begin{aligned} \Delta Q_{\Delta T} &= \frac{1}{2}\left[Q_{\Delta T}(\phi) - Q_{\Delta T}(-\phi)\right] \\ &= \frac{1}{2}\int \left[\mathcal{T}_{L,R} - \mathcal{T}_{R,L}\right](\epsilon - \mu_a) f_R d\epsilon \\ &+ \frac{1}{2}\int \left[\mathcal{T}_{L,P} f_P(-\phi) - \mathcal{T}_{P,L} f_P(\phi)\right](\epsilon - \mu_a)d\epsilon. \end{aligned} \tag{B4}$$

Linear response regime. We repeat the derivation of Sec. IV, and find that in the linear response regime, $\delta T_\nu / T_a \ll 1$, $T_L = T_a + \delta T_L$, $T_R = T_a + \delta T_R$, the probe temperature $T_P = T_a + \delta T_P$ obeys

$$\delta T_P(\phi) = \frac{\int d\epsilon \left(\frac{-\partial f_a}{\partial \epsilon}\right) \frac{(\epsilon - \mu_a)^2}{T_a} \left(\delta T_L \mathcal{T}_{L,P} + \delta T_R \mathcal{T}_{R,P}\right)}{\int d\epsilon \left(\frac{-\partial f_a}{\partial \epsilon}\right) \frac{(\epsilon - \mu_a)^2}{T_a} \left(\mathcal{T}_{P,L} + \mathcal{T}_{P,R}\right)} \tag{B5}$$

Using this relation, one can readily repeat the steps in Sec. IV and prove that $\mathcal{R}_{\Delta T} = 0$, thus $Q_{\Delta T}(\phi) = \mathcal{D}_{\Delta T}(\phi) = Q_{\Delta T}(-\phi)$.

Symmetry relations far from equilibrium. We discuss here symmetry relations for spatially symmetric junctions. We adapt the temperature probe condition (10) to three situations. First, the standard expression is given by

$$\begin{aligned} &\int d\epsilon (\mathcal{T}_{P,L} + \mathcal{T}_{P,R}) f_P(\phi)(\epsilon - \mu_a) \\ &= \int d\epsilon (\mathcal{T}_{L,P} f_L + \mathcal{T}_{R,P} f_R)(\epsilon - \mu_a). \end{aligned} \tag{B6}$$

We reverse the magnetic phase and get

$$\begin{aligned} &\int d\epsilon (\mathcal{T}_{L,P} + \mathcal{T}_{R,P}) f_P(-\phi)(\epsilon - \mu_a) \\ &= \int d\epsilon (\mathcal{T}_{P,L} f_L + \mathcal{T}_{P,R} f_R)(\epsilon - \mu_a). \end{aligned} \tag{B7}$$

Similarly, when interchanging the temperatures T_L and T_R we look for the probe distribution $\bar{f}_P$ which satisfies

$$\begin{aligned} &\int d\epsilon (\mathcal{T}_{P,L} + \mathcal{T}_{P,R}) \bar{f}_P(\phi)(\epsilon - \mu_a) \\ &= \int d\epsilon \left(\mathcal{T}_{L,P} f_R + \mathcal{T}_{R,P} f_L\right)(\epsilon - \mu_a). \end{aligned} \tag{B8}$$

Note that $f_P(\phi)$, $f_P(-\phi)$ and $\bar{f}_P(\phi)$ are required to follow a Fermi-Dirac form. The temperature β_P should be obtained so as to satisfy the probe condition. If the junction is left-right symmetric, the mirror symmetry $\mathcal{T}_{P,L}(\phi) = \mathcal{T}_{R,P}(\phi)$ applies. We use this relation in Eqs. (B7) and (B8) and conclude that the probe distribution obeys

$$\bar{f}_P(\phi) = f_P(-\phi). \tag{B9}$$

This directly implies that ($\mu_a = \mu_L = \mu_R = \mu_P$)

$$\bar{\beta}_P(\phi) = \beta_P(-\phi). \tag{B10}$$

Note that $\beta_P(\phi)$ does not need to obey any particular magnetic phase symmetry. The deviation from phase rigidity, Eq. (B4), can be expressed using the heat current flowing into the R terminal,

$$\begin{aligned} \Delta Q_{\Delta T} &= \frac{1}{2}\int (\epsilon - \mu_a)[(\mathcal{T}_{L,R} - \mathcal{T}_{R,L}) f_L \\ &- \mathcal{T}_{R,P} f_P(-\phi) + \mathcal{T}_{P,R} f_P(\phi)]d\epsilon. \end{aligned} \tag{B11}$$

We define $\Delta Q_{\Delta T}$ as the average of Eqs. (B4) and (B11),

$$\Delta Q_{\Delta T} = \frac{1}{4}\int d\epsilon(\epsilon-\mu_a)\Big[(\mathcal{T}_{L,R}-\mathcal{T}_{R,L})(f_L+f_R) + (\mathcal{T}_{L,P}-\mathcal{T}_{R,P})f_P(-\phi)+(\mathcal{T}_{P,R}-\mathcal{T}_{P,L})f_P(\phi)\Big].$$

Using the identities $\mathcal{T}_{L,R}-\mathcal{T}_{R,L}=\mathcal{T}_{P,L}-\mathcal{T}_{L,P}$ and $\mathcal{T}_{P,L}=\mathcal{T}_{R,P}$, the latter is valid in geometrically symmetric junctions, we get

$$\begin{aligned}&\Delta Q_{\Delta T}(\phi)\\ =\;&\frac{1}{4}\int(\mathcal{T}_{P,L}-\mathcal{T}_{P,R})(f_L+f_R-f_P(\phi)-\bar{f}_P(\phi))(\epsilon-\mu_a)d\epsilon\\ &=\mathcal{R}_{\Delta T}(\phi)=-\mathcal{R}_{\Delta T}(-\phi).\end{aligned}\quad\text{(B12)}$$

This concludes our derivation that under a temperature bias even (odd) heat conductance coefficients satisfy an odd (even) magnetic field symmetry,

$$\begin{aligned}\mathcal{R}_{\Delta T}(\phi) &= -\mathcal{R}_{\Delta T}(-\phi)=\Delta Q_{\Delta T}(\phi),\\ \mathcal{D}_{\Delta T}(\phi) &= \mathcal{D}_{\Delta T}(-\phi),\end{aligned}\quad\text{(B13)}$$

as long as the junction acquires a spatial mirror symmetry.

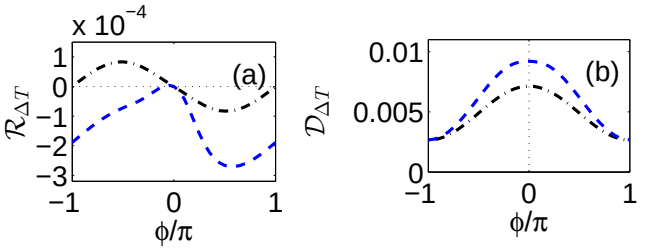

FIG. 14: Magnetic field symmetries of (a) even and (b) odd electronic heat conductance terms. Spatially symmetric system (dashed dotted), $\gamma_L=\gamma_R=0.05$. Spatially asymmetric junction (dashed), $\gamma_L=0.05\neq\gamma_R=0.2$. Light dotted lines represent the symmetry lines. Other parameters are $T_L=0.15$, $T_R=0.05$, $\epsilon_1=\epsilon_2=0.15$, $\gamma_P=0.1$, $\mu_a=\mu_L=\mu_R=\mu_P=0$.

We adopt the double-dot model (54) presented in Sec. VI and study its heat current behavior. In the absence of the probe, assuming for simplicity degeneracy and spatial symmetry, $\gamma/2=\gamma_{L,R}$, we obtain

$$Q_L(\phi)=\int d\epsilon(\epsilon-\mu_a)\frac{\gamma^2(\epsilon-\epsilon_d)^2\cos^2\frac{\phi}{2}}{\left[(\epsilon-\epsilon_d)^2-\frac{\gamma^2}{4}\sin^2\frac{\phi}{2}\right]^2+\gamma^2(\epsilon-\epsilon_d)^2}[f_L(\epsilon)-f_R(\epsilon)],$$

satisfying the Onsager symmetry. Fig. 14 displays the MF symmetries, and their violation, Deviations from phase symmetry for $\mathcal{D}_{\Delta T}$ are small, of the order of 10^{-5}.

[1] S. Andergassen, V. Meden, H. Schoeller, J. Splettstoesser, and M. R. Wegewijs, Nanotechnology **21**, 272001 (2010), and references therein.
[2] N. G. van Kampen, *Stochastic processes in physics and chemistry*, (North Holland, 1981).
[3] H.-P. Breuer and F. Petruccione, *The Theory of Open Quantum Systems* (Oxford University Press, Oxford, UK, 2002).
[4] M. Büttiker, Phys. Rev. B **32**, 1846 (1985); Phys. Rev. B **33**, 3020 (1986), IBM J. Res. Dev. **32**, 63 (1988).
[5] J. L. D'Amato and H. M. Pastawski, Phys. Rev. B **41**, 7411 (1990).
[6] T. Ando, Surf. Sci. **361-362**, 270 (1996).
[7] P. A. Jacquet, J. Stat. Phys. **134**, 709 (2009).
[8] K. Saito, G. Benenti, G. Casati, and T. Prosen, Phys. Rev. B **84**, 201306 (2011).
[9] V. Balachandran, G. Benenti, and G. Casati, Phys. Rev. B **87**, 165419 (2013).
[10] K. Brandner, K. Saito, and U. Seifert, Phys. Rev. Lett. **110**, 070603 (2013).
[11] J. P. Bergfield, S. M. Story, R. C. Stafford, and C. A. Stafford, ACS Nano **7**, 4429 (2013).
[12] Y. Ming, Z. Wang, Z. Ding, H. Li, New J. Phys. **12**, 103041 (2010).
[13] M. Bandyopadhyay and D. Segal, Phys. Rev. E **84**, 011151 (2011).
[14] E. Pereira, H. C. F. Lemos, and R. R. Avila, Phys. Rev. E **84**, 061135 (2011).
[15] Ph. A. Jacquet and C.-A. Pillet, Phys. Rev. B **85**, 125120 (2012).
[16] K. Saaskilahti, J. Oksanen, and J. Tulkki, Phys. Rev. E **88**, 012128 (2013).
[17] P. Roulleau, F. Portier, P. Roche, A. Cavanna, G. Faini, U. Gennser, and D. Mailly, Phys. Rev. Lett. **102**, 236802 (2009).
[18] M. J. M. de Jong and C. W. J. Beenakker, Physica A **230**, 219 (1996).
[19] S. A. van Langen and M. Büttiker, Phys. Rev. B **56**, R1680

(1997).
[20] H.-L. Engquist and P. W. Anderson, Phys. Rev. B **24**, 1151 (1981).
[21] D. Roy and A. Dhar, Phys. Rev. B **75**, 195110 (2007).
[22] F. Bonetto, J. Lebowitz, and L. Rey-Bellet, *Mathematical Physics 2000* (World Scientific, Singapore, 2000), pp. 128150.
[23] F. Bonetto, J. L. Lebowitz, and J. Lukkarinen, J. Stat. Phys. **116**, 783 (2004).
[24] A. Dhar and D. Roy, J. Stat. Phys. **125**, 801 (2006).
[25] D. Roy, Phys. Rev. E **77**, 062102 (2008).
[26] D. Segal, Phys. Rev. E **79**, 012103 (2009).
[27] S. Pilgram, P. Samuelsson, H. Förster, and M. Büttiker, Phys. Rev. Lett. **97**, 066801 (2006).
[28] L. Onsager, Phys. Rev. **37**, 405 (1931); **38**, 2265 (1931); H. B. G. Casimir, Rev. Mod. Phys. **17**, 343 (1945).
[29] Y. Imry, *Introduction to Mesoscopic Physics*, 2nd ed. (Oxford University Press, Oxford, 2002).
[30] A. Yacoby, M. Heiblum, D. Mahalu, and H. Shtrikman, Phys. Rev. Lett. **74**, 4047 (1995).
[31] H. Linke, W. D. Sheng, A. Svensson, A. Löfgren, L. Christensson, H. Q. Xu, P. Omling and P. E. Lindelof, Phys. Rev. B. **61**, 15914 (2000).
[32] A. Löfgren, C. A. Marlow, I. Shorubalko, R. P. Taylor, P. Omling, L. Samuelson, and H. Linke, Phys. Rev. Lett. **92**, 046803 (2004).
[33] C. A. Marlow, R. P. Taylor, M. Fairbanks, I. Shorubalko, and H. Linke, Phys. Rev. Lett. **96**, 116801 (2006).
[34] J. Wei, M. Shimogawa, Z. Wang, I. Radu, R. Dormaier, and D. H. Cobden, Phys. Rev. Lett. **95**, 256601 (2005).
[35] R. Leturcq, D. Sanchez, G. Götz, T. Ihn, K. Ensslin, D. C. Driscoll, and A. C. Gossard, Phys. Rev. Lett. **96**, 126801 (2006); R. Leturcq, R. Bianchetti, G. Götz, T. Ihn, K. Ensslin, D.C. Driscoll, and A. C. Gossard, Physica E **35**, 327 (2006).
[36] D. M. Zumbhl and C. M. Marcus, M. P. Hanson and A. C. Gossard, Phys. Rev. Lett. **96**, 206802 (2006).
[37] L. Angers, E. Zakka-Bajjani, R. Deblock, S. Gueron, H. Bouchiat, A. Cavanna, U. Gennser, and M. Polianski, Phys. Rev. B **75**, 115309 (2007).
[38] M. Sigrist, T. Ihn, K. Ensslin, M. Reinwald, and W. Wegscheider, Phys. Rev. Lett. **98**, 036805 (2007); T. Ihn, M. Sigrist, K. Ensslin, W. Wegscheider, and M. Reinwald, New J. Phys. **9**, 111 (2007).
[39] G. M. Gusev, Z. D. Kvon, E. B. Olshanetsky, and A. Y. Plotnikov, Europhys. Lett. **88**, 47007 (2009).
[40] F. G. G. Hernandez, G. M. Gusev, Z. D. Kvon, J. C. Portal, Phys. Rev. B **84**, 075332 (2011).
[41] D. Sanchez and M. Büttiker, Phys. Rev. Lett. **93**, 106802 (2004); M. Büttiker and D. Sanchez, Int. J. Quantum Chem. **105**, 906 (2005).
[42] B. Spivak and A. Zyuzin, Phys. Rev. Lett. **93**, 226801 (2004).
[43] A. R. Hernandez and C. H. Lewenkopf, Phys. Rev. Lett. **103**, 166801 (2009).
[44] J. S. Lim, D. Sanchez, and Rosa Lopez, Phys. Rev. B **81**, 155323 (2010). Note that in this work the authors used a different convention for the current expansion with voltage, $I = G_0\Delta\mu + G_1\Delta\mu^2 + ...$
[45] T. Kubo, Y. Ichigo, and Y. Tokura, Phys. Rev. B **83**, 235310 (2011).
[46] V. Puller, Y. Meir, M. Sigrist, K. Ensslin, and T. Ihn, Phys. Rev. B **80**, 035416 (2009).
[47] M. Terraneo, M. Peyrard, G. Casati, Phys. Rev. Lett. **88**, 094302 (2002); D. Segal, A. Nitzan, ibid. **94**, 034301 (2005); C. W. Chang et al., Science **314**, 1121 (2006).
[48] X.-F. Li, X. Ni, L. Feng, M.-H. Lu, C. He, and Y.-F. Chen, Phys. Rev. Lett. **106**, 084301 (2011).
[49] L. Feng, Y.-L. Xu, W. S. Fegadolli, M.-H. Lu, J. E. B. Oliveira, V. R. Almeida, Y.-F. Chen, and A. Scherer, Nature Materials **12**, 108 (2013).
[50] S. Bedkihal, M. Bandyopadhyay, and D. Segal, Phys. Rev. B **88**, 155407 (2013).
[51] R. Landauer, IBM J. Res. Dev. **1**, 223 (1957).
[52] M. Büttiker, Phys. Rev. Lett. **57**, 1761 (1986).
[53] S. Datta, *Electric transport in Mesoscopic Systems* (Cambridge: Cambridge University Press 1995).
[54] W. H. Press, B. P. Flannery, S. A. Teukosky, and W. T. Vetterling, *Numerical Recipes in C: The Art of Scientific Computing*, (Cambridge University Press 1992).
[55] Persistent currents exist in at thermal equilibrium due to the absence of time-reversal symmetry. In our work here we consider only net charge transport. However, since persistent currents are antisymmetric in the magnetic field, we could add them to the defintion of $\mathcal{R}(\phi)$, and our observations would be still valid.
[56] Y. Meir and N. S. Wingreen, Phys. Rev. Lett. **68**, 2512 (1992).
[57] J. Fransson, *Non-equilibrium nano-physics, a many body approach* Lecture Notes in Physics **809**, Springer (2010).
[58] S. Bedkihal and D. Segal, Phys. Rev. B **85**, 155324 (2012).
[59] M. W.-Y. Tu, W.-M. Zhang, J. Jin, O. Entin-Wohlman, and A. Aharony, Phys. Rev. B **86**, 115453 (2012).
[60] S. Bedkihal, M. Bandyopadhyay, and D. Segal, Phys. Rev. B **87**, 045418 (2013).
[61] B. Kubala and J. König, Phys. Rev. B **65**, 245301 (2002).
[62] S. Bedkihal and D. Segal, unpublished.
[63] E. Deyo, B. Spivak, and A. Zyuzin, Phys. Rev. B **74**, 104205 (2006).
[64] A. Ueda and M. Eto, Phys. Rev. B **73**, 235353 (2006); New J. Phys. **9**, 119 (2007).
[65] T. Kubo, Y. Tokura, and S. Tarucha, J. Phys. A: Math. Theor. **43**, 354020 (2010).
[66] D. Sanchez and K. Kang, Phys. Rev. Lett. **100**, 036806 (2008).
[67] V. I. Puller and Y. Meir, Phys. Rev. Lett. **104**, 256801 (2010).
[68] O. Hod, R. Baer, and E. Rabani, Phys. Rev. Lett. **97**, 266803 (2006).
[69] O. Hod, R. Baer, and E. Rabani, J. Phys. Condens. Matter **20**, 383201 (2008).
[70] O. Entin-Wohlman and A. Aharony, Phys. Rev. B **85**, 085401 (2012).
[71] K. Saito and Y. Utsumi, Phys. Rev. B **78**, 115429 (2008).
[72] D. Sanchez and R. Lopez, Phys. Rev. Lett. **110**, 026804 (2013); S.-Y. Hwang, D. Sanchez, M. Lee, and R. Lopez, arXiv: 1306.6558v1.
[73] D. Sanchez and L. Serra, Phys. Rev. B **84**, 201307(R) (2011).
[74] R. S. Whitney, Phys. Rev. B **87**, 115404 (2013).
[75] Z. Zimboras, M. Faccin, Z. Kadar, J. D. Whitefield, B. P. Lanyon, and J. Biamonte, Scientific Reports **3:2361**, 1 (2013).
[76] V. Kashcheyevs, A. Aharony, and O. Entin-Wohlman, Phys. Rev. B **73**, 125338 (2006).